Forecasting Research

Forecasting Research Division
Technical Report No. 43

Development of the surface data assimilation scheme for the new mesoscale model

by

A J Maycock

April 1993

Meteorological Office
London Road
Bracknell
Berkshire
RG12 2SZ
United Kingdom

FORECASTING RESEARCH TECHNICAL REPORT NO 43

Development of the surface data assimilation scheme for the new mesoscale model

by

A J Maycock

April 1993

ABSTRACT

The development of the scheme for the pre-processing, quality control, and assimilation of surface observations in the new mesoscale model (NMM) is described. This includes the use of extra surface data types (screen temperatures and 10m winds over land), and hourly rather than three hourly observations. The synoptic impact on a rapidly intensifying low case is shown. Experiments were performed on two further cases for the tuning of assimilation parameters. It is shown that 10m winds over land have only a small impact during assimilation, with no impact in the forecasts. The impact of screen temperature data is beneficial well into the forecast. Future work on surface data assimilation in the NMM is briefly discussed.

Forecasting Research Division,
Meteorological Office,
London Road,
Bracknell,
Berkshire RG12 2SZ,
United Kingdom.

1. Introduction

The decision to replace the Meteorological Office's previous operational mesoscale model (Golding 1990) with a mesoscale version of the Unified Model (Cullen 1991) required a revision of the pre-processing, quality control, and assimilation of surface data. The increased resolution, both in the horizontal and vertical, and the shorter model timestep, meant that many of the parameters appropriate to the global and limited area configurations of the model would not be appropriate to the mesoscale version. This technical note describes the work done to devise a suitable scheme for the new mesoscale model (NMM), and how it differs from the existing global and limited area (LAM) models. The NMM was implemented operationally, with the changes described in this report, in December 1992.

The finer resolution of the mesoscale version of the Unified Model also meant that there was a potential benefit from using a greater density of data than is used in the Limited area and Global configurations. It was hoped that use could be made of more surface data types in the NMM, and with surface data valid at each hour. In the LAM, surface data is extracted at three hourly intervals. It was anticipated that land screen temperature observations and 10m wind observations over land would have an impact; these data types are not used in the LAM assimilation. The NMM uses the same Analysis Correction data assimilation scheme (Lorenc, Bell, and Macpherson 1991) as the existing Unified Model configurations. Details of the NMM are given in Ballard and Robinson (1993).

2. Pre-processing

A study into the quality of synop screen temperature and ten metre wind data in the mesoscale area was made using data stored in the Limited Area Model Observation Processing Database (OPD). The aim of these studies was ultimately to produce a list of stations whose data were considered to be consistently of a low quality - or unrepresentative of the model gridbox - and to reject them permanently from the mesoscale version.

The study was made using three months worth of data (independently) ; July, November, and December 1991. The LAM OPD contains data for approximately 400 stations in the NMM domain. Although 10m winds and 1.5m temperatures are not used in the LAM assimilation, they undergo quality control procedures so that their quality can be monitored. By using the quality control information which is stored in the OPD, for each station within the mesoscale area several monthly statistics were obtained:

i) The percentage of observations flagged;
ii) The mean (O-A) and (O-B) errors;
iii) The standard deviations of these errors.

The studies into 10m winds and 1.5m temperatures are individually described below.

2.1 10m winds

It was clear that there were certain stations which were consistently having a high observation rejection rate. Many of these were in the mountainous areas within the mesoscale domain (Scotland and French/Swiss border). This is due to the local orography of these stations which the LAM does not resolve, and although the LAM data is a good place to start a study such as this, it must be remembered that the greater resolution of the NMM will hopefully lead to improved wind forecasts in such areas.

Care was taken to decide which criteria should cause a station to be "blacklisted". The mean error statistics were used to identify stations where there was a bias, and the standard deviation figures were used to spot stations whose observations differed from the LAM analysis (or background) with large variability. Values chosen in the production of these synop wind blacklists were as follows :

i) A rejection rate of 5% or above;
ii) A monthly mean (O-A) or (O-B) of 2.5 ms^{-1} or above (in the wind vector);
iii) A standard deviation in these errors of 5 ms^{-1} or above.

Choosing a final list of stations whose 10m wind reports were to be permanently rejected was not easy. Many stations featured in, say, one of the blacklists but not in the other two. Also, stations may have seemed particularly poor in one of the months, yet have next to no rejections in the other two. In order to produce a reasonably sized blacklist, it was found necessary to modify the criteria that had been set. Having looked at the statistics for the three months, it was decided to base the blacklist mainly on rejection rate statistics; stations featuring on more than one month were ranked higher on the blacklist. The result was a list of the worst 80 stations in the NMM domain in terms of LAM quality control decisions.

The locations of these stations are shown in Fig 1.

2.2 1.5m temperatures

An identical study to the one described above was made for screen temperature data over land. The same statistics were calculated for each station, and they were sorted to produce screen temperature blacklists. However, it was found to be much more difficult to create an overall blacklist that would be beneficial to include into the NMM quality control. The individual station observation rejection rates varied considerably from month to month, as did the mean and standard deviations of the errors.

Taking 5% to be an unacceptable observation rejection rate meant that only about 1% of stations (i.e. about 4) would have been blacklisted in each month; however no station fell into a blacklist on more than one month. The value of 5°C (two times an assumed observation error) was taken as the cut-off for an acceptable value of the standard deviation of (O-B). During the three months studied (i.e a total of about 1200 stations in the NMM area), only 4 exceeded this value. For each of these stations, the value was unusually high in one month and low in the other two. The data for two of these stations was investigated in detail. It was found that a high proportion of their reports were defective. Investigations made through OP Division showed this to be due to a problem with the automatic recording equipment, which was consistently leading to reports of -30.0°C

The study of the land screen temperature data led to the conclusion that no benefit would be obtained from blacklisting any station's reports. However, the study did lead to further investigation into many stations with large mean (O-B) and (O-A) errors. These were found mainly to be in mountainous areas. The large discrepancies between station height and model orographic height in these areas were causing these errors, and an investigation was made into the effect of using a standard lapse rate correction to the observed temperatures. Examples from the original study are shown below :

STATION	Station height (m)	Model height (m)	Difference (m)	Monthly mean (O-A) (°C)
06791	3299	2135	1164	-6.9
16008	1461	2379	-918	+7.3
06792	1706	2293	-587	+3.4

For the case when model orography height is greater than station height, the model background will be too cold. The figures above are consistent with this, and the values agree well with a lapse rate of -6.5°C/km.

The same study of temperature errors with the same data was made, only this time a correction factor C was *added* to the observed screen temperature. This is given below :

$$C = -\Gamma(h_m - h_s)$$

where : Γ is a standard lapse rate of -6.5°C per kilometre;
h_m is the LAM orographic height;
h_s is the station height.

The results of adding this correction were very encouraging. For all the months studied, the RMS errors were reduced by a significant amount. In December, the reduction in RMS was about 7%, in July and September it was 18%. In all the months the mean error was made 0.19°C more negative. This is a consequence of the average model height in the area being studied being 30m higher than the average station height.

For September's data, the effect of this lapse rate correction was evaluated for each of the eight analysis times in the day, to check that it had no negative impact at certain times. It was found to have a good impact on the RMS errors at each of the analysis hours. The size of the impact was found to be virtually independent of analysis time. The results of adding this lapse rate correction are shown in Fig. 2.

This correction has been added operationally to the LAM pre-processing step.

2.3 Observation errors

Assuming that observation and model background errors are independent, then the following relationship should hold,

$$\overline{(o-b)^2} \approx e_o^2 + e_b^2$$

where o is an observed value, b a model background value, e_o^2 is the observation error variance (including the error of representativeness) and e_b^2 is the model background error variance. An overbar denotes averaging.

Initial results for the NMM gave values for the left hand side of the above relationship smaller than the sum of error variances, indicating that the specified errors for the LAM were too large for the NMM. This may be expected, to some extent, because the smaller NMM gridbox would lead to a smaller error of representativeness.

The observation errors for the NMM have been reduced from 2.5 to 2.0 ms^{-1} for the 10m wind components, and from 2.5 to 2.0°C for screen temperatures. [N.B. Since this study, the 10m wind observation error in the LAM has been reduced to 1.7 ms^{-1}

because of a change to 10m wind background errors; this change has not yet been made in the NMM].

3. Surface data assimilation

3.1 Preliminary investigations.

A suitable case for the investigation of the impact of extra surface data was chosen; this was the development of an intense low over Southern Ireland on the 12th November 1991 (Heming 1992). The case was chosen partly because of the failure of the LAM to develop the depression sufficiently. The synoptic situations at 12Z and 18Z are shown in Fig. 3. At 12Z, there was a closed circulation over Southern Ireland with a central pressure of 974mb. By 18Z this had moved north eastwards to the East Scottish coast, and had a central pressure of 959mb. The operational LAM 12Z analysis is shown in Fig. 4a and the T+6 forecast from this is shown in Fig. 4b. It can be seen that the model did not show any sign of the closed circulation and subsequently the forecasts were poor.

Several NMM runs were made for this case. These were nominal 12Z data time runs (i.e. assimilation observation files at 09Z and 12Z). The aim was to look just at the synoptic impact of using the extra surface data; no objective verification of the forecasts was done.

The first run of the NMM for this case was to demonstrate the impact of the finer resolution of this configuration. The same data as used in the LAM were used in this run; i.e three hourly surface data, and no extra data types. The same assimilation parameters as used in the LAM were also used. Figs. 5a and 5b show the 12Z and 18Z charts from this run. It can be seen that the extra model resolution alone has produced sharper troughing both at analysis time and in the T+6.

The next run (Figs. 5c and 5d) again used the same data types, but this time surface observations (MSLP and ship winds) were extracted hourly. The extra data alone has had no marked impact on either the analysis or the forecast. A further run with hourly surface data was made, but this time the length of the insertion period for surface data was reduced, in keeping with the higher frequency of data. In the LAM (and in the previous NMM run), observations are assimilated over a period from 2½ hours before their valid time to ½ hour after - a total of 3 hours. For the next NMM run the time window for assimilation of the surface data was reduced to 1½ hours before, ¼ hour after. The resulting analysis and T+6 forecast are shown in Figs. 5e and 5f. Again, little impact was seen in the pressure patterns.

In Heming(1992) several LAM reruns were performed to determine the cause of the poor analysis. It was found that the greatest impact was obtained in a run with a bogus radiosonde ascent to support the Valentia (S.W. Ireland) ascent. Operationally, the lowest 10 LAM level winds were flagged, in the rerun with the bogus just three mid-level winds were flagged. In order to obtain maximum impact with the NMM, a dummy radiosonde ascent was set up with the observed winds interpolated onto the NMM levels. The next NMM run was as the previous one (hourly surface data, shorter insertion period), but with the bogus Valentia radiosonde winds. The charts are shown in Figs. 4c and 4d. The effects on both the analysis and forecast were good. In both the trough is much sharper, and although no closed circulation was produced, there were spot lows of 981mb and 965mb respectively. This is a much more accurate picture than that predicted by the LAM in its corresponding rerun.

In keeping with the greater density of surface data being used in these runs, a run was made in which the correlation scale of the model forecast error was reduced. The (LAM) values previously used were correlation scales of 300/190/210 km. at start of insertion period/observation time/end of insertion period. For the next NMM run these values were reduced to 270/170/185 km. The effect of this (Figs. 5g and 5h) was to slightly increase the troughing, although the impact was not large.

A run was made in which observations of 10m winds over land were used. This is not done in the LAM. Again, hourly observations were used with a reduced insertion period, but the default correlation scale was used. This did have a slight positive impact (Figs. 5i and 5j), the troughing is slightly sharper again. In the 18Z chart, the 966mb line (e.g.) extends further south, and the spot low is also moved further south to roughly its correct position.

In order to obtain the maximum impact from the NMM, a further "best" run was made. This included the following :

- All surface data hourly;
- Further reduced correlation scale (225/150/165 km);
- Further reduced time window (-1¼ hours,¼ hour);
- Improved LAM boundary conditions (from a LAM run with the bogus Valentia ascent assimilated).

The resulting 12Z and 18Z MSLP charts are shown in Figs. 5k and 5l. It can be seen that at 12Z the 980mb line has been brought much further south relative to the initial run, and although there is no closed circulation the spot low has been reduced to 979mb. At 18Z the impact of the data is still there, and there is now a closed circulation in the correct place.

In order to determine how much of the impact can be attributed to the extra surface data alone, a "control run" was performed. This had all the extra surface data taken out (i.e. no synop wind observations and 3 hourly surface pressure observations). The assimilation time window was increased back to the LAM value. The improved LAM boundary conditions and the bogus Valentia upper air winds were left in. PMSL difference charts valid at 18Z showing the impact of the extra surface data alone, and the impact of the finer model resolution alone, are shown in Figs. 5m and 5n

By studying Fig. 5o, it is clear that the surface data has had a beneficial impact in the forecast. It resulted in sharper troughing, with the production of a closed low at T+6. As reported in the case study (Heming 1992), in cases like this upper air data can have a much greater influence than surface data on the surface pattern. The Valentia ascent in this case had the greatest impact. However, we have obtained a definite impact with the use of more surface data, this was further investigated with more detailed tuning experiments, and experiments to investigate the impact of using observations of screen temperature over land.

3.2 Tuning of assimilation parameters

Experiments to fine-tune the surface data assimilation parameters were performed on two different cases chosen from those selected for the trial of the NMM. These were :

i) DT 0Z 23/08/91 - "Spiral vortex" case;
ii) DT 0Z 04/12/91 - Anticyclonic/stratocumulus case.

Initial tuning was done with runs for both cases, using hourly extracted surface data (P. and 10m winds only).
The preliminary tuning involved finding suitable values for the three major parameters that determine the way in which the observations are used in the assimilation. These are :

i) The time window for assimilation;
ii) The radius of influence of the observations;
iii) The forecast error correlation scale.

Initially, a control run was made for each case. The parameters used in this were based on results from the 12/11/91 case. The values, along with their corresponding LAM values, are given below :

PARAMETER	Value in control run	Value in LAM
Correlation scale (C.S)	225/150/165 km	300/190/210 km
Radius of influence	1.75 x C.S 3.5 for ship winds	3.5 x C.S
Time window	(-75,15) minutes (2x for ship winds)	(-150,30) minutes

Three tuning runs were then made on each case. These involved changing one of the parameters from its control run value, whilst leaving the other two as before. The three tuning runs differed from the control run in the following way :

RUN 1) Radius of influence varied. Parameters as control run but with radius of influence changed to 2.5 × C.S. for all surface data.

RUN 2) Correlation scale varied. Parameters as control run but with correlation scale changed to (270/170/190) km for all surface data.

RUN 3) Time window varied. Parameters as control run but with assimilation time window changed to (-120,24) minutes for all surface data.

Both the fit to observations during assimilation and forecast verifications were looked at for each of the runs - we desire an improvement in both these results as there is a danger of drawing the model too close to the observations during assimilation and compromising any potential improvements in forecast skill. The value of RMS $\partial P_*/\partial t$ over the model domain was also monitored. Too high a value for this indicates gravity wave activity; i.e. forcing the observations in too strongly.

The RMS (observation-model) increments for surface pressure and 10m winds are shown in Fig. 6.

By comparing the time window run with the control run, it seems that the time window chosen initially for the assimilation of hourly surface pressure and 10m wind data was too short. In the run with the time window increased to (-120,24) minutes, the fit during to the P. observations was improved. In the anticyclonic case, the fit was better than or the same as in the control run in 19 of the 22 timesteps studied. In the spiral vortex case, the fit was better than or the same in 16 of the 22 timesteps. The forecast verifications (in PMSL) were also better at least out to T+12, with no impact in the 10m wind forecasts. Increasing the time window also led to improvements in the fit to 10m wind observations during assimilation. In the anticyclonic case the fit was better than or the same as the control run in 18 of the 22 timesteps, and 16 in the spiral vortex case. The fit was also better at the end of each 3 hour assimilation cycle. The positive impact seen in the fit to observations during assimilation does not seem to last very far into the forecast however, only a slight impact is seen in the PMSL verification, and virtually none in the 10m wind forecasts.

Increasing the radius of influence (relative to the control run) led to a poorer fit to the P. observations. In the spiral vortex case, the RMS error was, on average, about 10 to 15% higher. A worsening in the fit to 10m wind observations over land was also observed - particularly in the spiral vortex case. The fit to ship 10m winds was slightly improved in this run.

Increasing the correlation scale, both for surface pressure and 10m winds, led to a much poorer fit to observations during assimilation.

The results from the four preliminary runs led to a set of improved assimilation parameters for surface data. A further run, designed to incorporate all the improvements found above, was made, in which the time window of (-120,24) mins. was used, a correlation scale of (225/150/165) km., and a radius of influence of 2.5 correlation scales was used for ship winds (1.75 for other surface data). The results from this run showed that the overall fit to land surface data benefited from the longer time window than that used in the control run. However, the fit to ship winds was worse than in the test run. (This may suggest that the improvement in the fit to ship winds in the radius of influence run was not a result of reducing the ship wind radius of influence, but a result of increasing the radius of influence for land 10m winds). Thus, a final set of parameters that obtains maximum impact from the extra surface data being used was arrived at; these are given in table 1. Fig. 7 shows the fit during assimilation to observations for three runs; the original control run, the new 'best' run (using the parameters from table 1), and the 'best' run without synop wind data assimilated. This shows the impact of using the tuned parameters, and the impact of using synop wind data.

3.2.1 Weighting of geostrophic wind increments.

In order to try and improve the fit to 10m wind observations, and possibly retain some of the impact in the forecasts, runs were made in which less weighting was given to the geostrophic wind increments. These increments are calculated to balance geopotential increments resulting from the assimilation of mass field information. The geostrophic wind increment can be expressed as :

$$\delta' v_m = 1/f\ k \wedge \nabla \delta \Phi_m$$

where f is the Coriolis parameter;
$\delta\Phi_m$ is the geopotential increment

Only a fraction of this increment is added, however. A weighting is given, which depends on three scaling factors. These are a hemisphere dependent term (due to the higher number and quality of wind observations in the northern hemisphere); a level dependent term (due to the geostrophic relationship being less accurate at low levels); and a latitude dependent term. In the global model this term must be zero at the equator where the geostrophic relationship is not valid, and rise to one at the poles. In the limited area model, the fraction of the increment applied is 0.5 at all points in the domain.

An experiment was run (using the two cases described above) in which this weighting was reduced to 0.25, prompted by the higher resolution of the NMM. The result of this was to improve the fit to 10m winds, but worsen the fit to surface pressures during assimilation. There was only a very slight impact in the 10m wind forecasts, and a slight decline in the PMSL forecasts. At timesteps 120 and 240 (the nominal analysis times), the improvements in the fit to 10m winds were about 1.8% and 1.1% respectively. The decline in the fit to P. observations was about 2.7% and 1.4% respectively. The benefits in the wind field do not justify the lower weighting value due to the unacceptable degradation in the surface pressure field. This experiment justifies retaining the LAM value for weighting the geostrophic wind increments in the NMM.

3.2.2 **Nudging of observations.**

In an attempt to retain some of the impact from data in forecasts of 10m winds, the assimilation was re-run with an increased nudging coefficient for surface winds. By forcing the model to draw nearer to observations during the assimilation period, it was hoped that the resulting model forecast would retain this impact when assimilation ceased. Using the same two cases as before, the best assimilation parameters were used and the nudging coefficient was increased by 35% (from 5.55556×10^{-4} to 7.50×10^{-4}). The results, both from the fit to observations during assimilation and the forecast verification, showed that both the mean windspeed error and RMS wind vector error were reduced during the assimilation. The reduction in RMS vector error was about 2%. However, verification of the T+3 forecasts (1½ hours after the end of assimilation) showed that no impact whatsoever was retained in the windspeed or RMS vector error scores.

3.2.3 Use of synop temperature data.

Using the two cases described above, similar preliminary NMM assimilation runs as described in section 3.2 were run, but with observations of screen temperature over land included in the assimilation. The parameters used in the assimilation were the same as those used in the previous 'best' run. Runs without synop temperatures, with synop temperatures, and with synop temperatures assimilated over 1 level only (as opposed to the entire 10 level boundary layer) were made. The results showed that much more impact, not only during assimilation but also well into the forecast, was obtained compared to our experiments with synop winds. The fit to observations during assimilation and the verification scores are shown in Fig. 8 for the anticyclonic case. The same trends are observed in the spiral vortex case but to a lesser degree. It is clear that we have a significant and long lasting effect - in the anticyclonic case the RMS differences are 0.7, 0.5, and 0.3°C lower at 3, 6, and 9 hours *into the forecast*.

The same assimilation was rerun with synop temperatures, but including a modification to the assimilation scheme in which the surface temperature T_* is incremented by the same amount as the atmospheric level 1 temperature. This was only done for land points - sea surface temperatures were not updated in this way. The results from this, shown in Fig. 9, show that another large and positive impact was obtained, both in the RMS fit to screen temperatures and the forecast verifications. More work could be done along this line - at present the T_* increments are not fed down to the lower soil levels.

3.2.4 Vertical weighting of increments

Referring to Fig. 9, it can be seen that there was little difference in the fit to screen temperature observations, during assimilation, between the runs in which the temperature increments were added over 1 and 10 levels. In the forecast scores, the 10 level run was better. However, particularly in the anticyclonic December case, it was found that the 10 level run fitted worse to radiosonde temperatures and cloud observations. This is of concern in the December case when operationally the forecast of stratocumulus coverage was poor anyway. At three hours into the assimilation, the RMS fit to sonde temperatures was around 0.2°C worse - which is smaller than the benefit obtained for screen temperatures. However, the cloud forecasts (Fig. 10) are found to be worse in runs with synop temperatures assimilated, particularly over 10 levels. This may be due to the fact that the cloud layer was very low and shallow in this case, possibly having a cloud top height below level 10.

To try and retain the large impact of synop temperature assimilation seen in screen temperature scores, but reduce the problems of degrading the cloud forecasts and fit to upper air temperatures, experiments were made in which the vertical profile of the increment weighting was altered. We do not wish to confine the increments to the lowest level only, but at the same time we have found that adding too large an increment at higher levels has a detrimental effect. A compromise is to change the vertical correlation scale, which controls the rate at which the increment weighting decreases with pressure. The equation giving the correlation between the increments at two levels P_L and P_M (where $P_L > P_M$) is :

$$\ln \mu_v = \{-b \ln^2(P_L/P_M)\}$$

The value of b controls the rate at which the correlation tails off with height - its value in the LAM and global configurations is 3.0. A NMM assimilation was run in which this value was increased to 6.25^2. Fig. 11 shows the difference in vertical correlation profiles.

With the sharper profile it was found that the screen temperature verification scores were only slightly worsened in the December case, and there was a slight improvement in the fit to all observation types - particularly P_*. The cloud forecast (Fig. 12) was also better in the 'large b' run, looking more like the 1 level run in this respect.

Having verified further runs with different combinations of number of analysis levels and vertical correlation profiles, the current operational NMM has 6 analysis levels for screen temperatures, and a b value of 13.75^2 (see Fig.11).

4. Summary and conclusions.

The assimilation of extra surface data in the higher resolution mesoscale Unified Model has resulted in positive impacts. We have found that an increase in the frequency of data used had a small positive synoptic impact in the 12/11/91 case. The assimilation of 10 metre winds over land has achieved an improvement during assimilation, but as yet no worthwhile impact in the forecasts. The assimilation of screen temperature data over land has resulted in a large impact during assimilation and well into the forecast, with a further improvement coming when the surface temperature field over land was updated at each timestep. By adjusting the vertical profile of the increment weighting, any degradation to the upper air temperatures and cloud forecasts was largely avoided.

5. Future work.

The revision to the pre-processing of surface wind observations (e.g. the production of a blacklist of stations for 10 metre winds) was based on studies of LAM data. It may be that a similar study using operational NMM data, which was not available at the time, would lead to a revision of these results, as the model will hopefully have better background 10 metre wind fields because of the more detailed orography. These studies can be repeated once sufficient NMM statistics have accumulated in the OPD.

The experiments investigating the impact of assimilating synop winds and temperatures will, in the future, be repeated using screen relative humidity data. This is with a view to improving low cloud and visibility forecasts - products for which the mesoscale model is intended to give useful guidance.

References

Ballard, S.P. and Robinson, R., 1993, 'Development and performance of the new mesoscale model.' Forecasting Research Technical Report No. 40.

Cullen, M.J.P., 1991, 'The unified forecast/climate model.' Short-range Forecasting Research Sci. Paper No. 1.

Golding, B., 1990, 'The Meteorological Office mesoscale model.' Meteorol. Mag., **119**, 81-96.

Heming, J.T., 1992, 'The Development of a Small Intense Depression over Southern Ireland 12 November 1991.' Central Forecasting Case Study No. 30.

Lorenc, A.C., Bell, R.S. and Macpherson, B., 1991, 'The Meteorological Office analysis correction data assimilation scheme.' Q.J.R. Meteorol. Soc., **117**, 58-89.

Acknowledgements

I would like to thank Dr. B. Macpherson for his guidance throughout the whole of this project, and the modelling section of the mesoscale group; Sue Ballard, Richard Barnes, Bob Robinson, Simon Jackson, and Steve Woltering. Numerous other people, from both FR division and CF division, also provided valuable help.

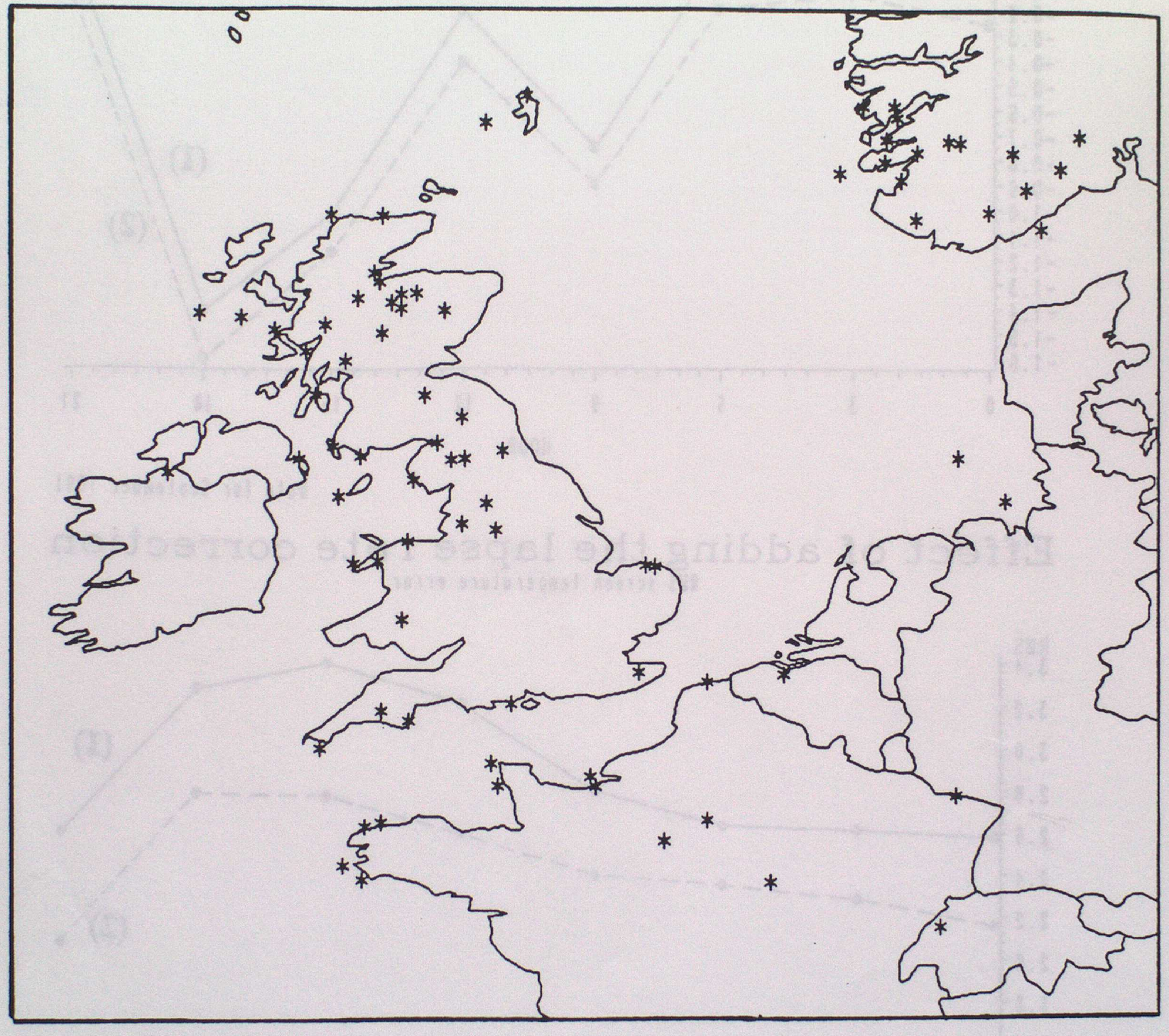

Fig. 1 Locations of stations whose 10m wind observations are not used in the NMM.

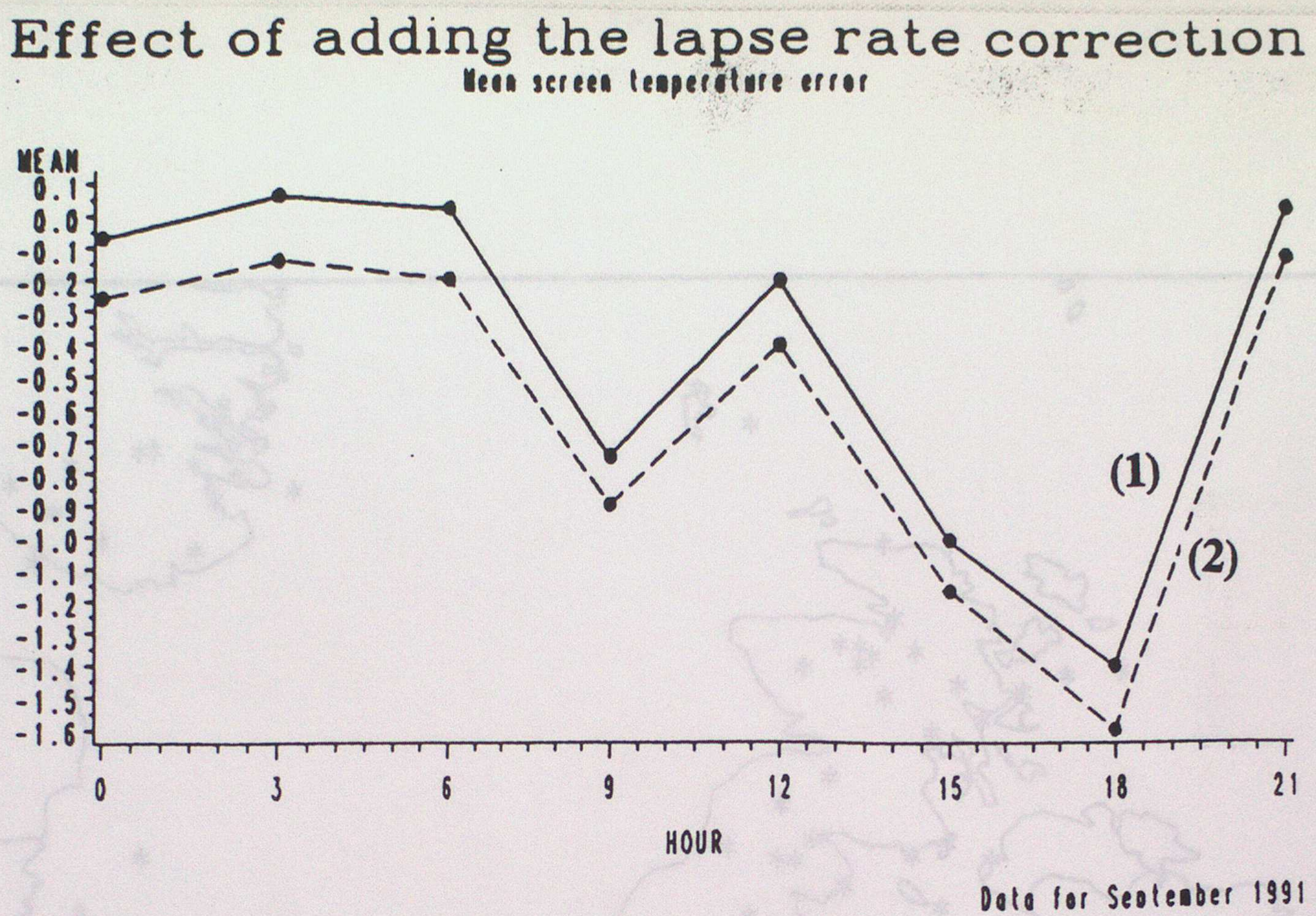

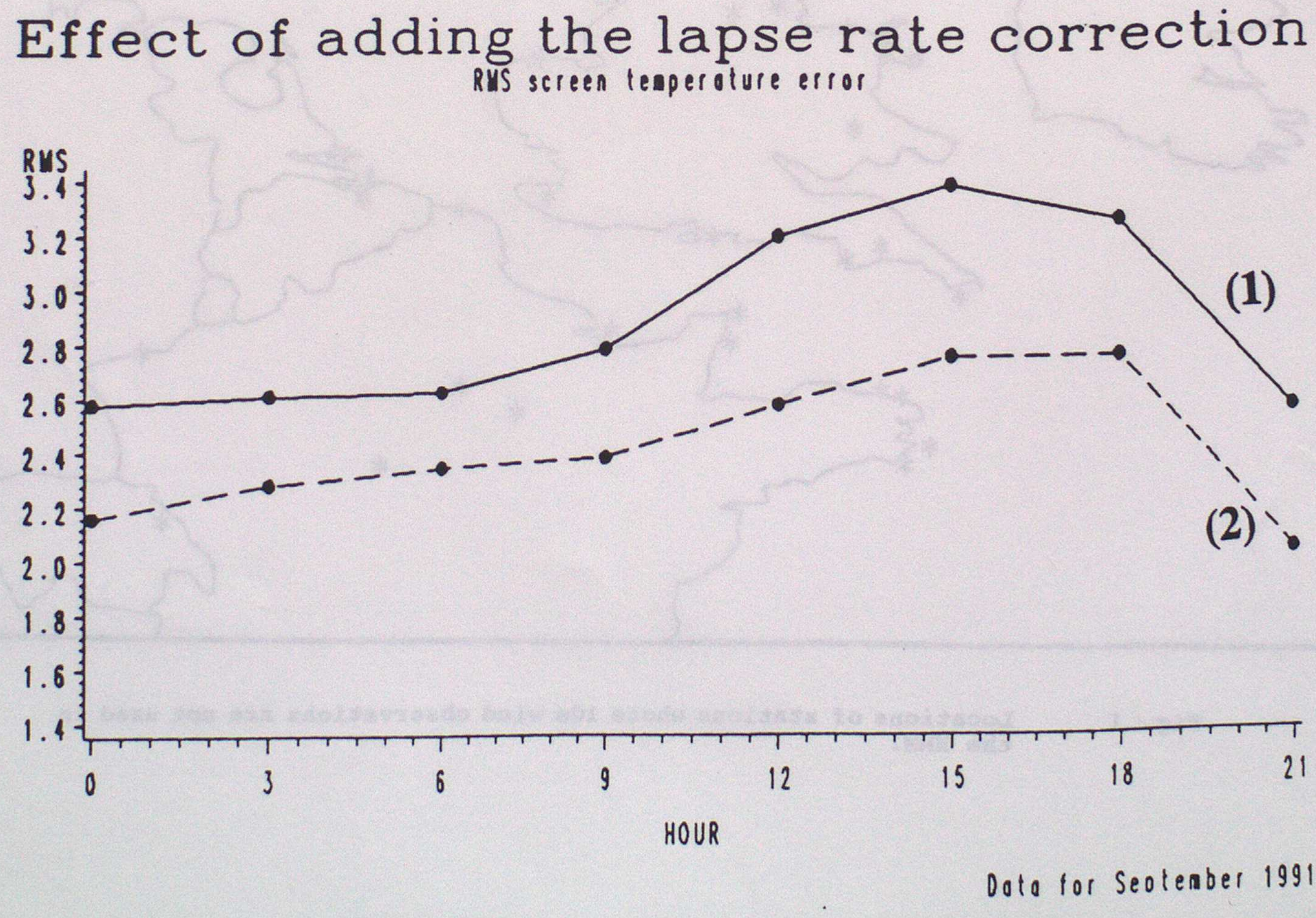

Fig. 2 Screen temperature errors with and without the lapse rate correction applied. (1) without correction ; (2) with correction.

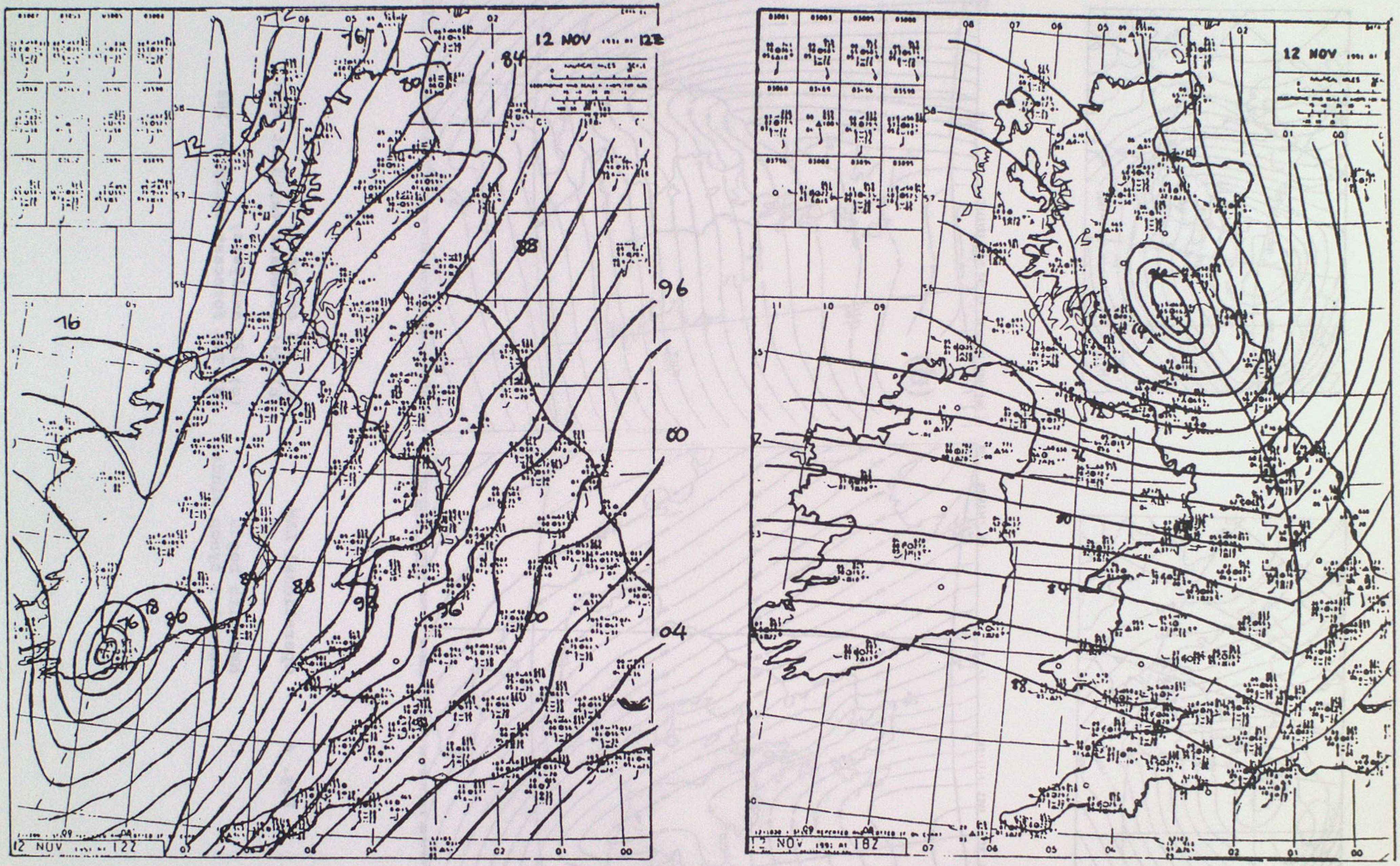

Fig. 3 Hand drawn analyses at 12 and 18Z 12/11/1991.

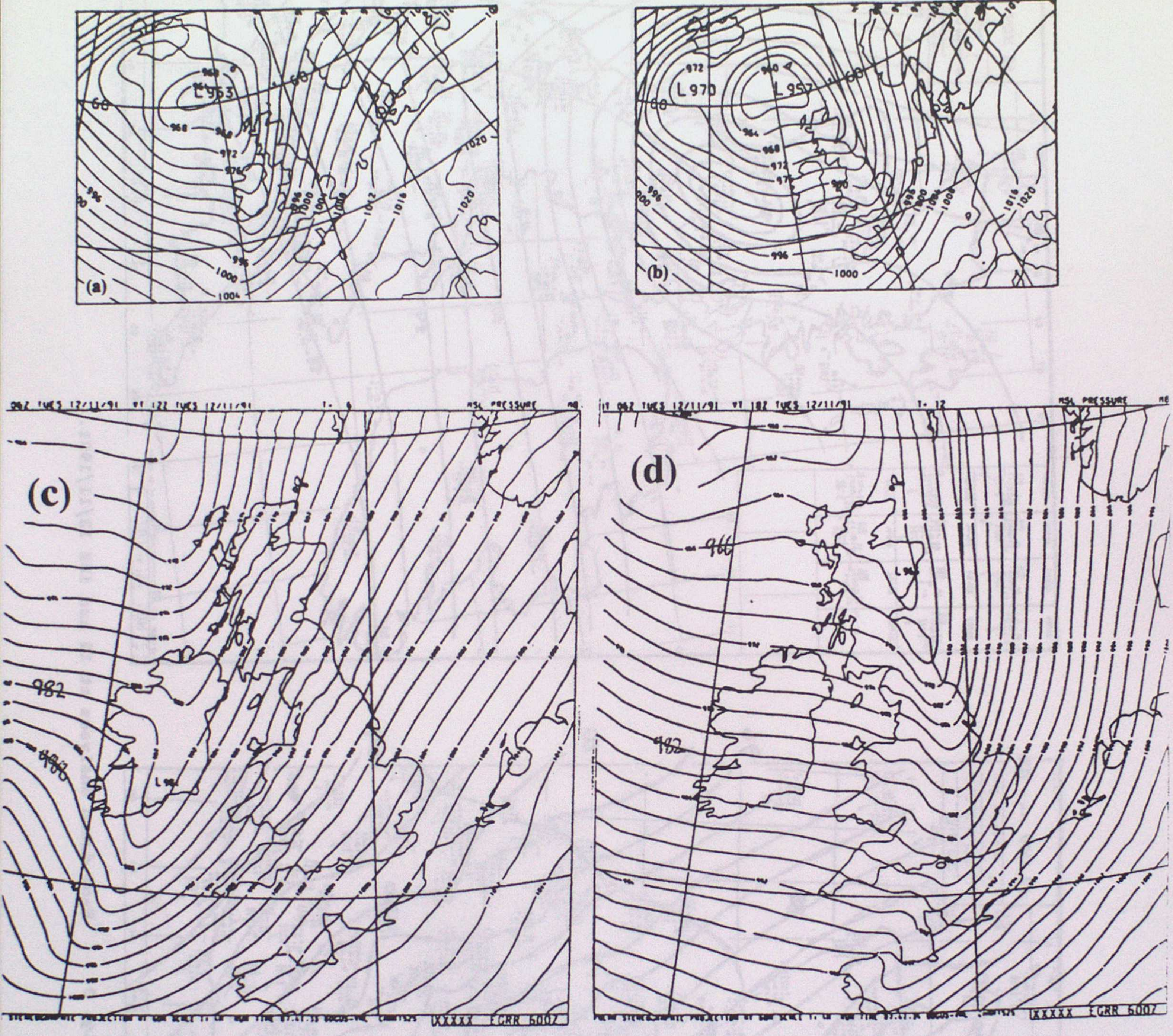

Fig. 4 Operational LAM (a) 12Z analysis;
(b) T+6 forecast valid at 18Z.

NMM with bogus ascent + synop winds (c) 12Z analysis;
(d) T+6 forecast valid at 18Z.

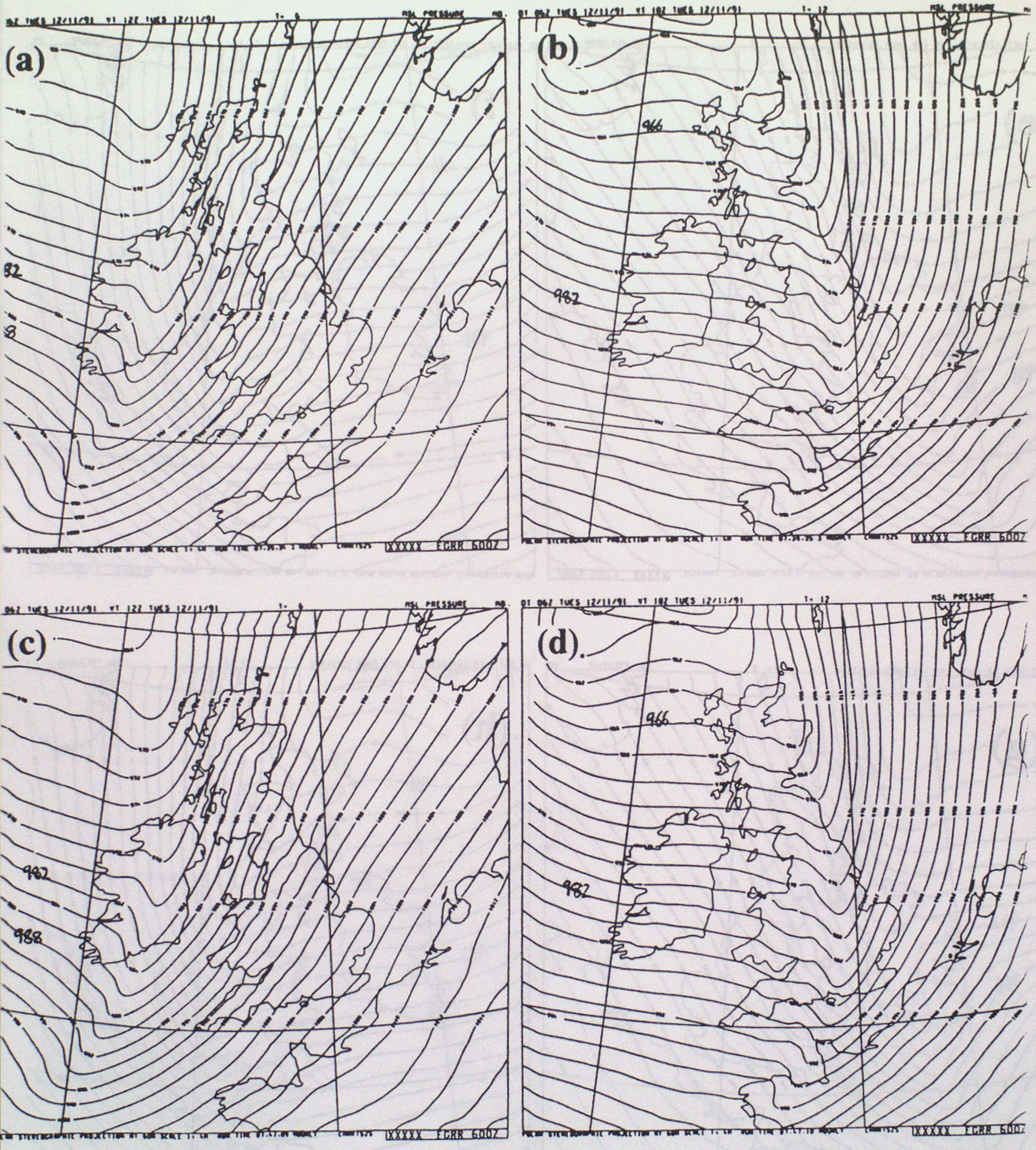

Fig. 5 NMM analysis (on left) and T+6 forecasts (on right) from :
(a),(b) run with standard LAM data and assimilation parameters;
(c),(d) as above but with hourly surface data.

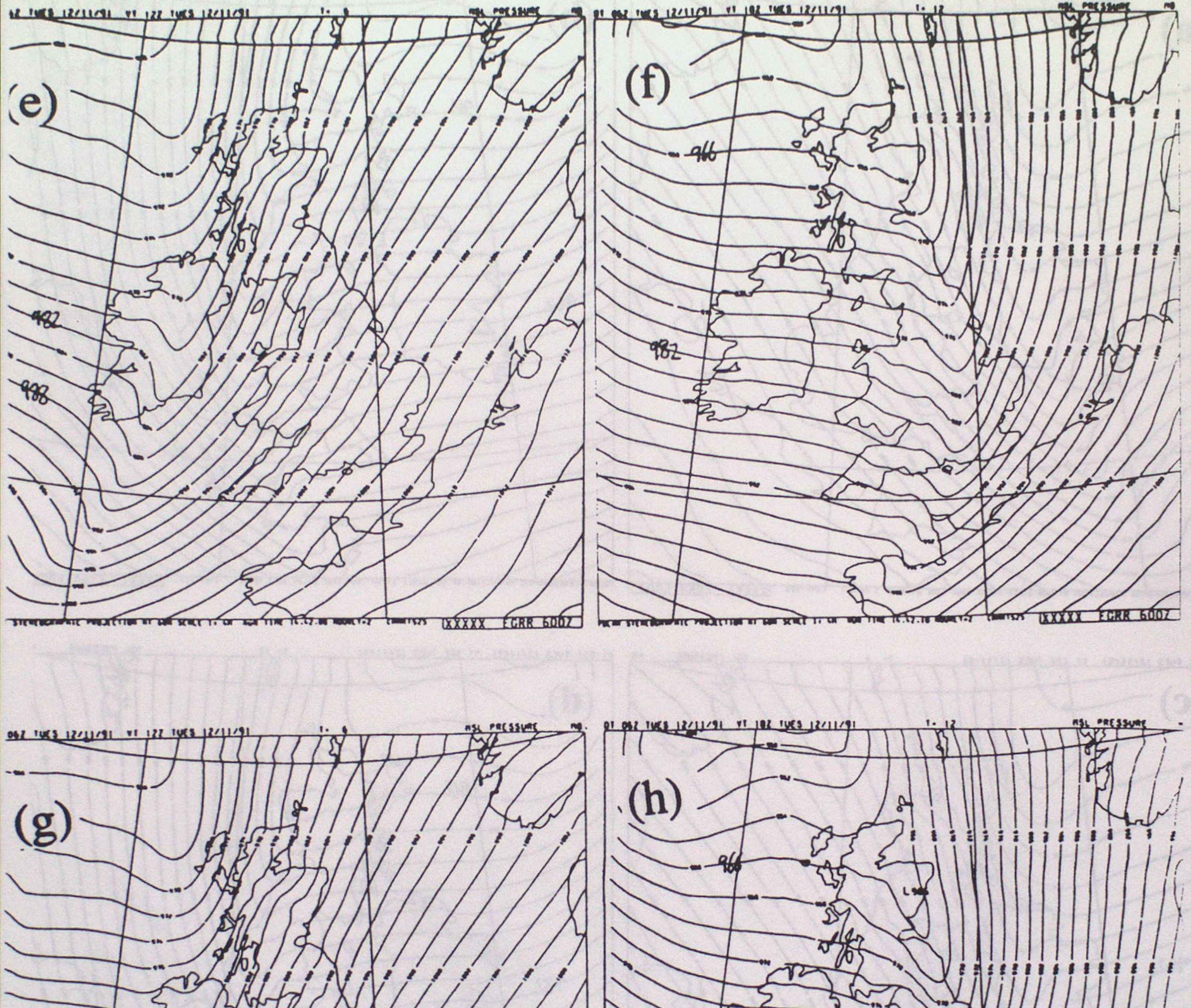

Fig. 5 cont..

NMM analysis (on left) and T+6 forecasts (on right) from :
(e),(f) run with hourly surface data and reduced insertion time window;
(g),(h) run in which forecast error correlation scale was reduced;

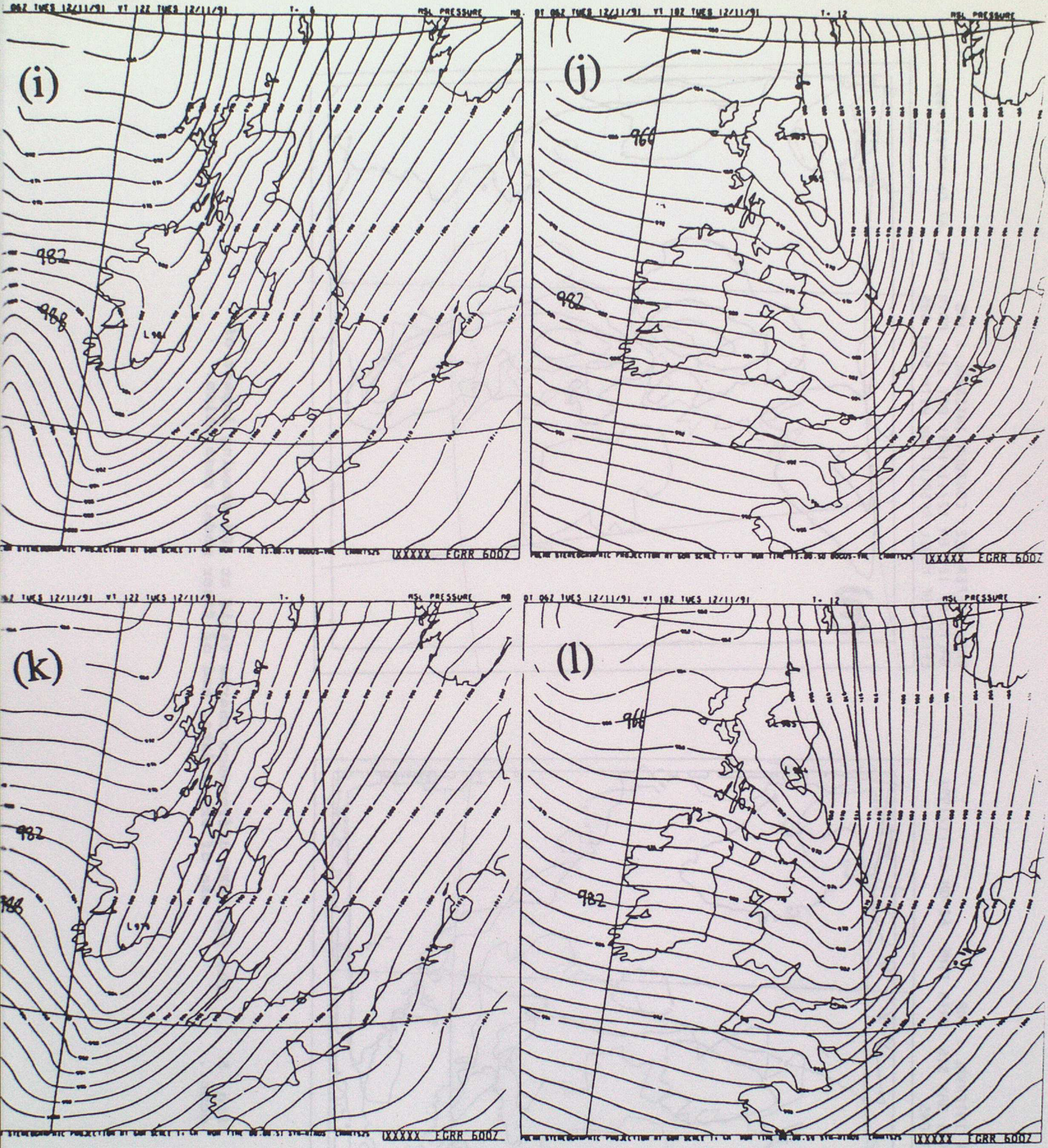

Fig. 5 cont.. NMM analysis (on left) and T+6 forecasts (on right) from :
(i),(j) as (4c) and (4d) but with synop winds assimilated.
(k),(l) best run based on previous runs;

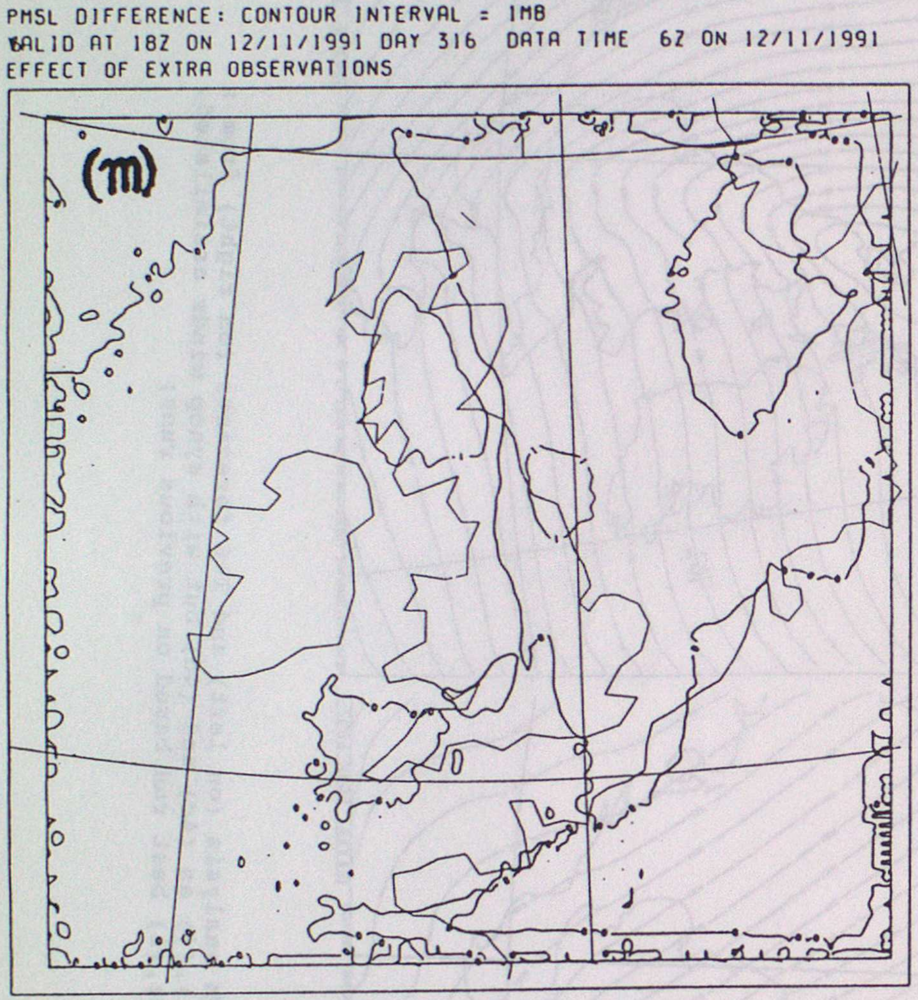

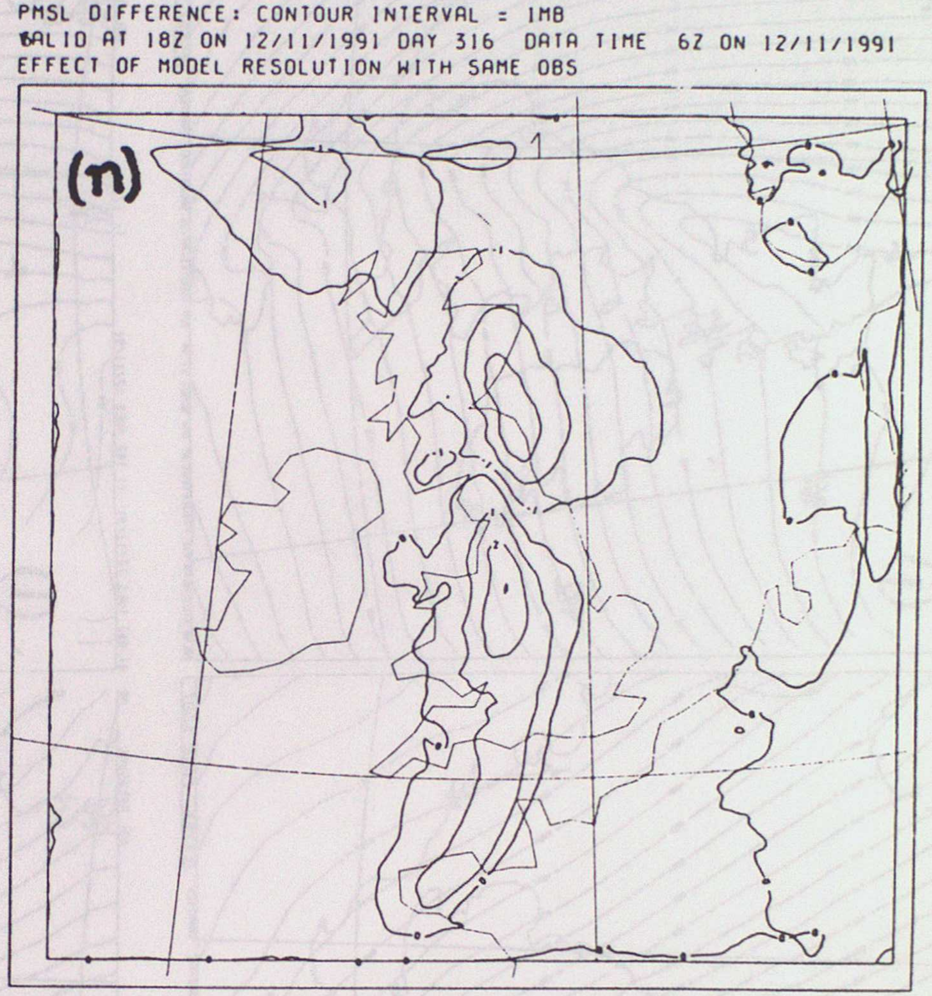

Fig. 5 cont.. (m),(n) PMSL difference charts valid at 18Z showing impact of use of extra data, and of finer model resolution.

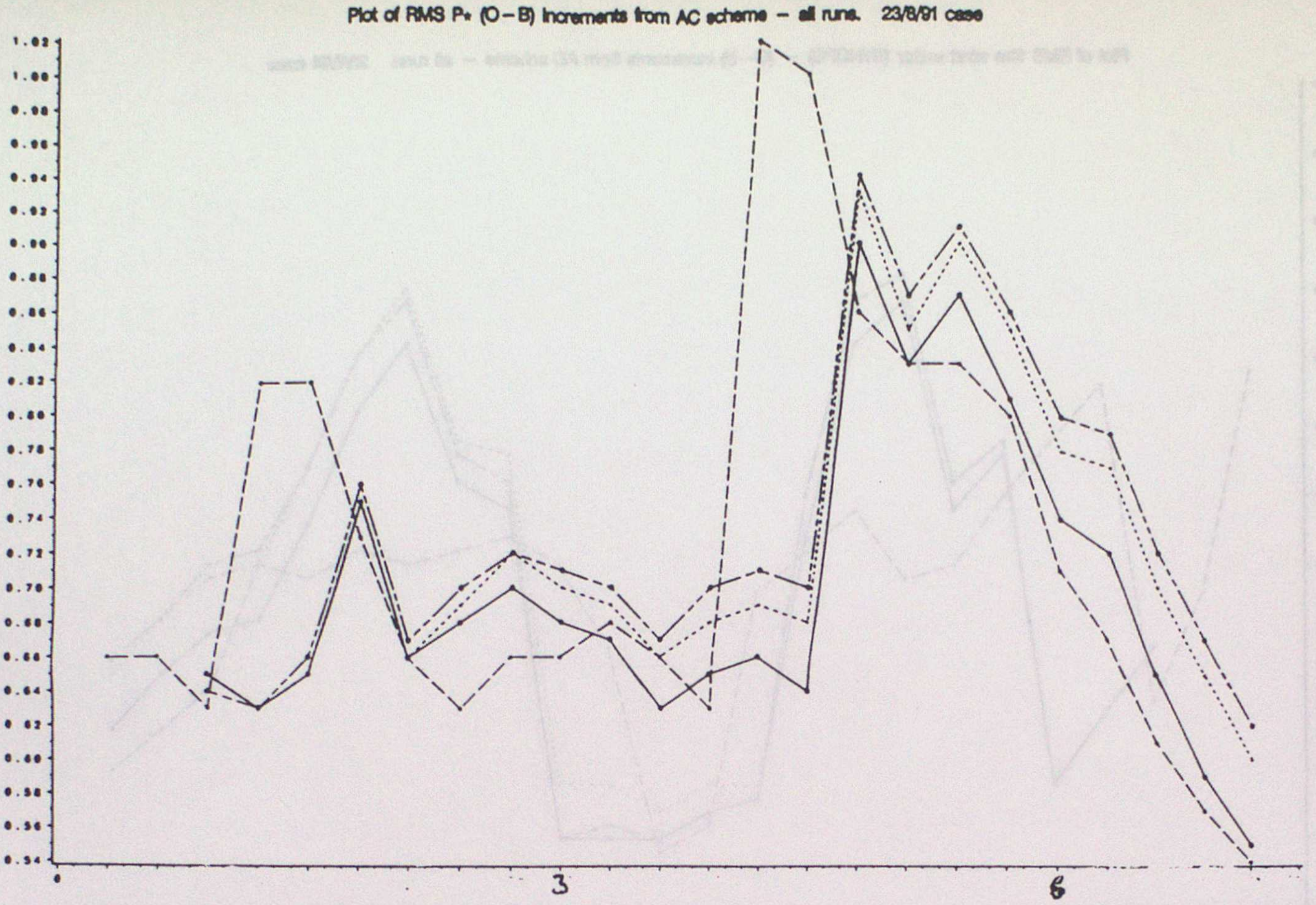

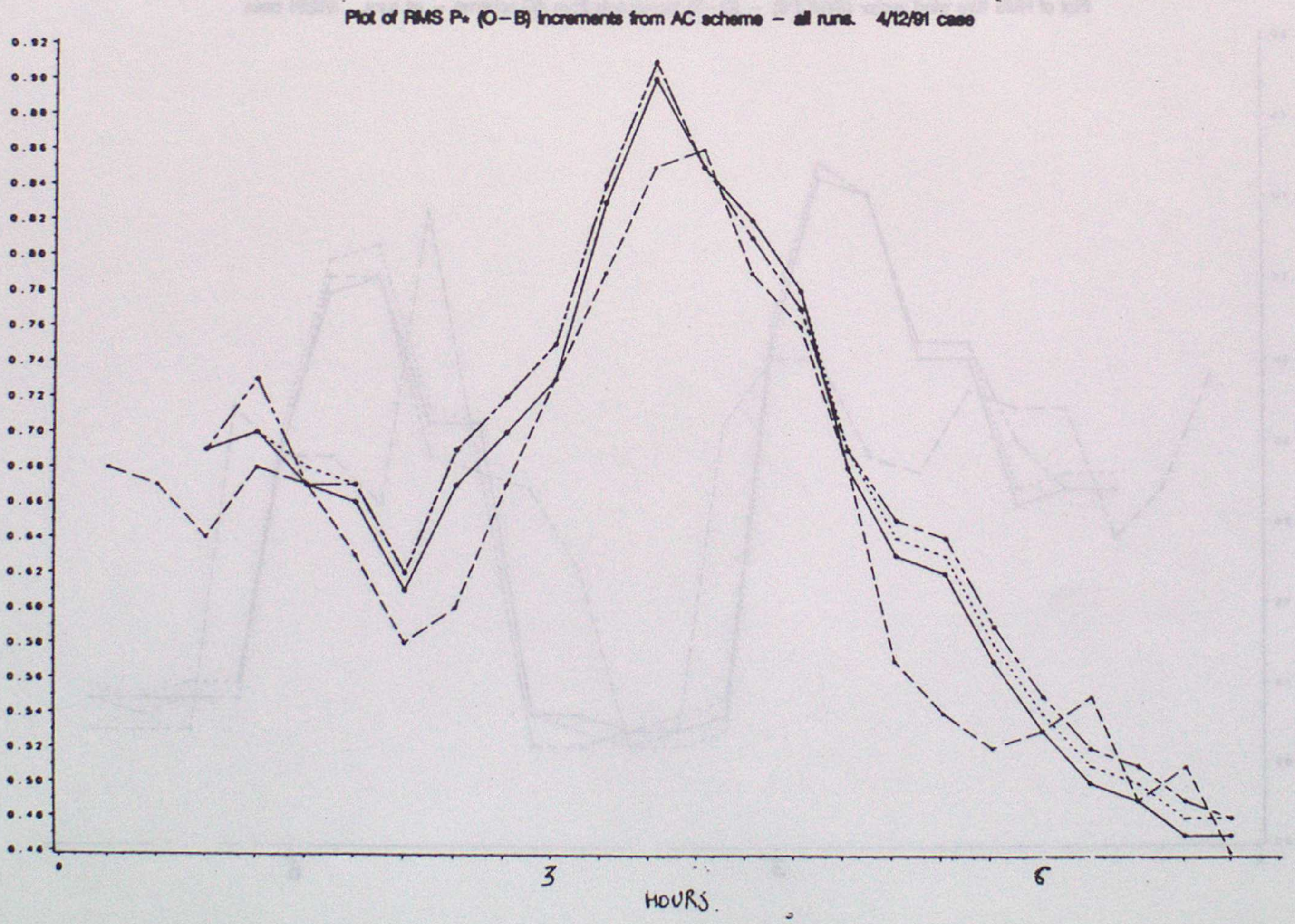

Fig. 6 **Fit to P* and 10m winds during assimilation**

KEY : solid line - control run
dotted line - increased radius of influence run
dashed line - increased time window run
chained line - increased correlation scale run.

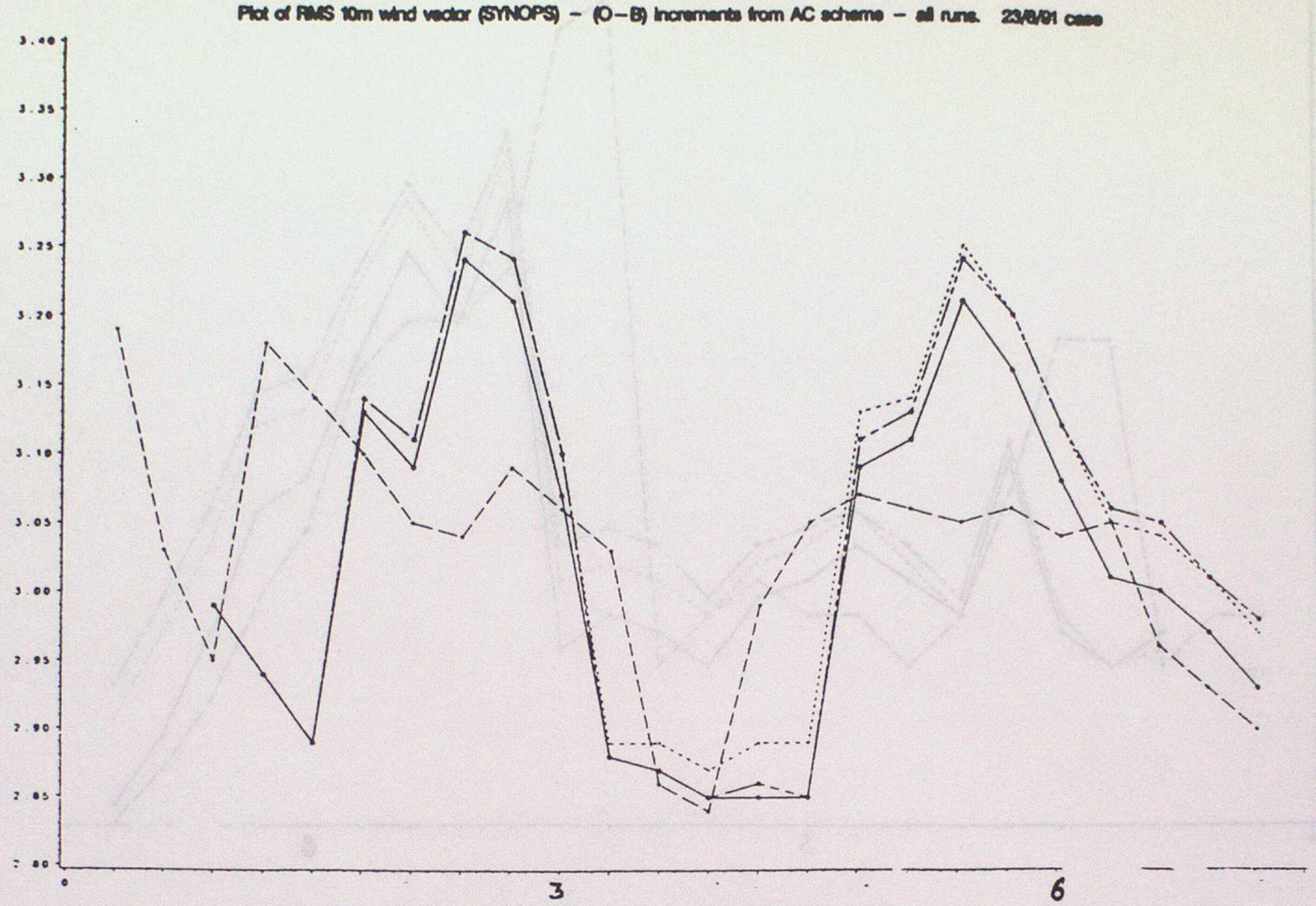

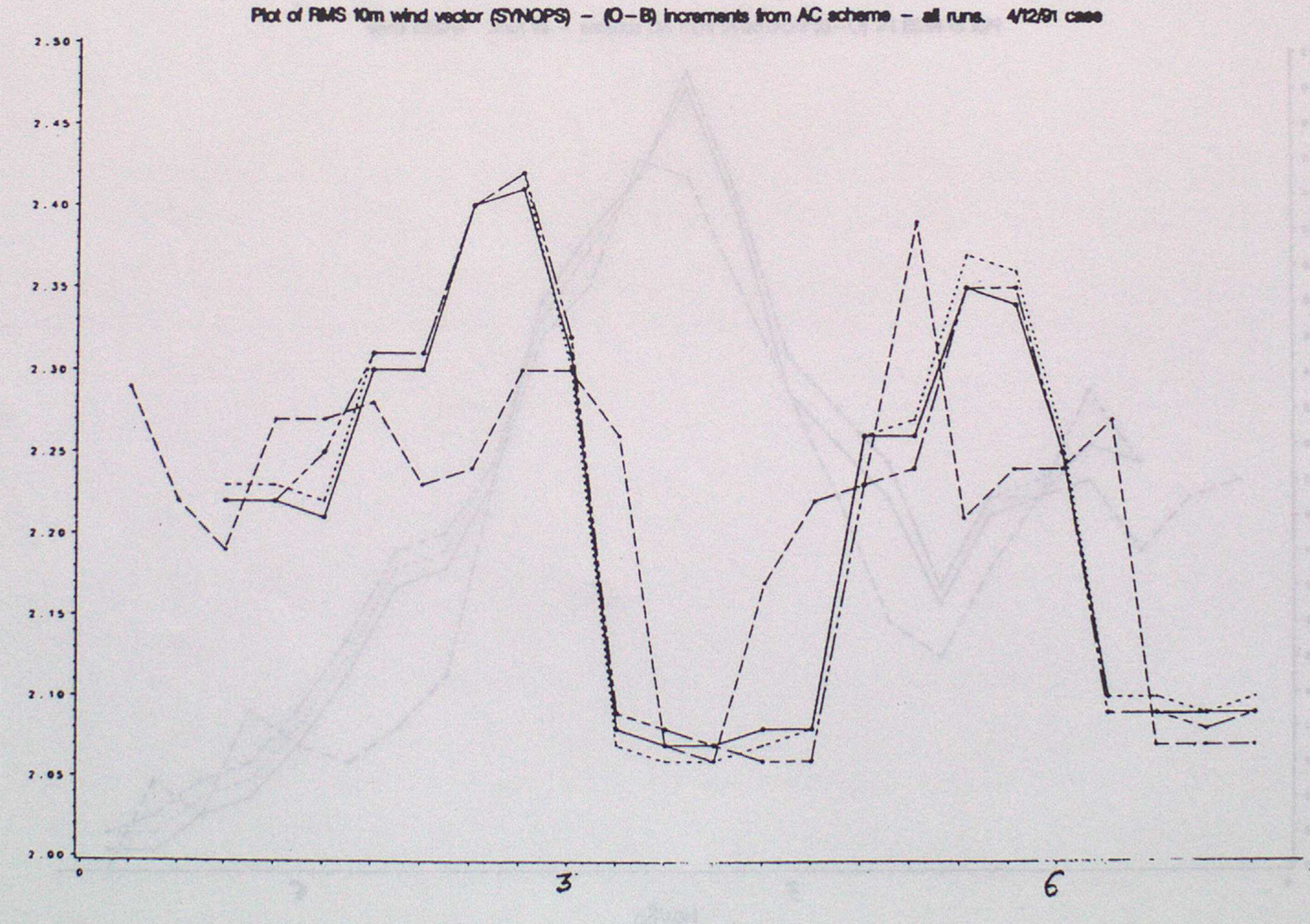

Fig. 6 Fit to P* and 10m winds during assimilation

KEY : solid line - control run
dotted line - increased radius of influence run
dashed line - increased time window run
chained line - increased correlation scale run.

Plot of RMS (O-B) 10m wind increments from AC scheme - all runs 23/8/91 case

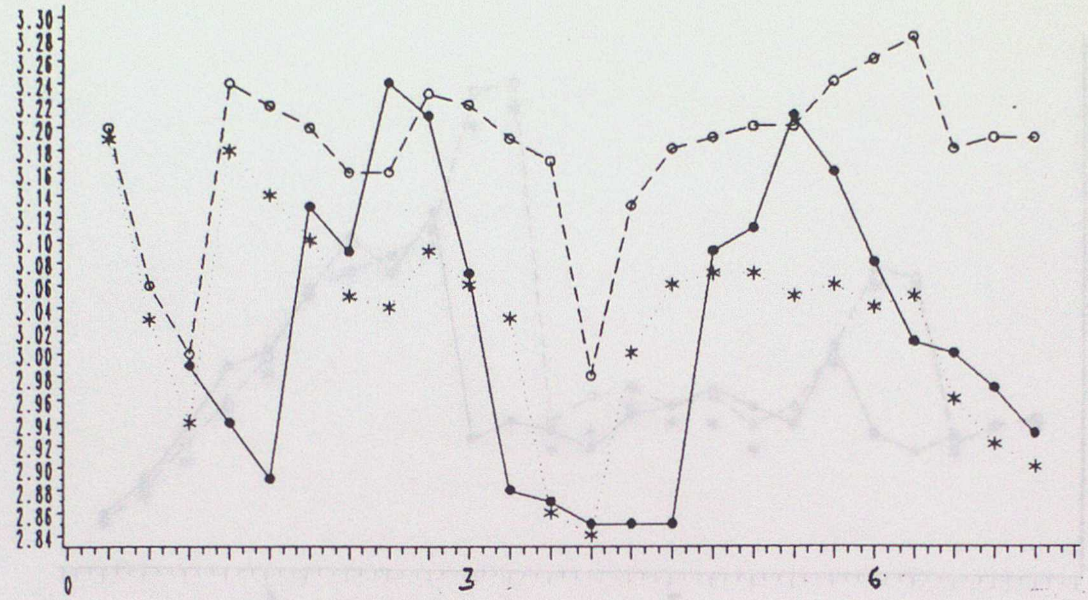

Plot of RMS (O-B) 10m wind increments from AC scheme - all runs 4/12/91 case

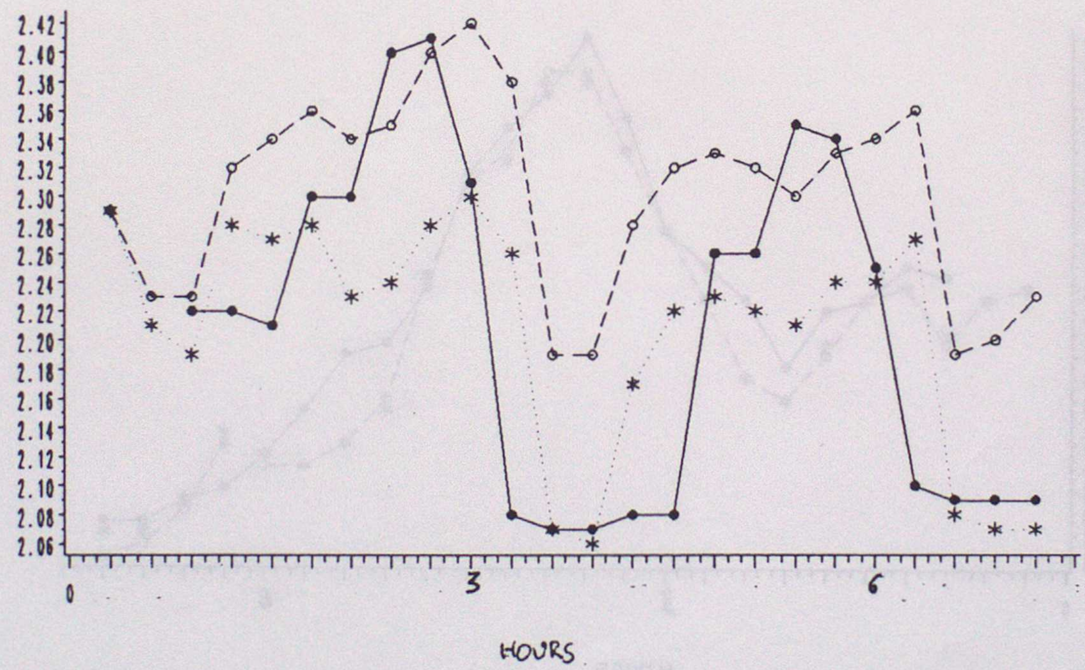

Fig. 7 Fit to P* and 10m winds during assimilation

KEY : stars - 'best run'
hollow circles - no synop winds
filled circles - original control

Plot of RMS (0-B) P* increments from AC scheme - all runs 23/8/91 case

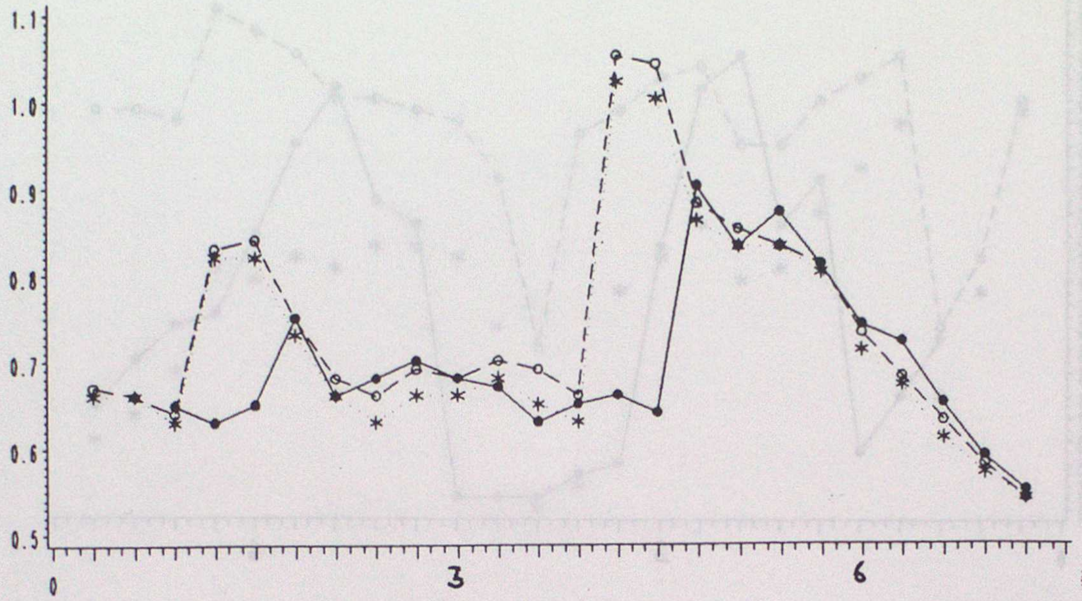

Plot of RMS (0-B) P* increments from AC scheme - all runs 4/12/91 case

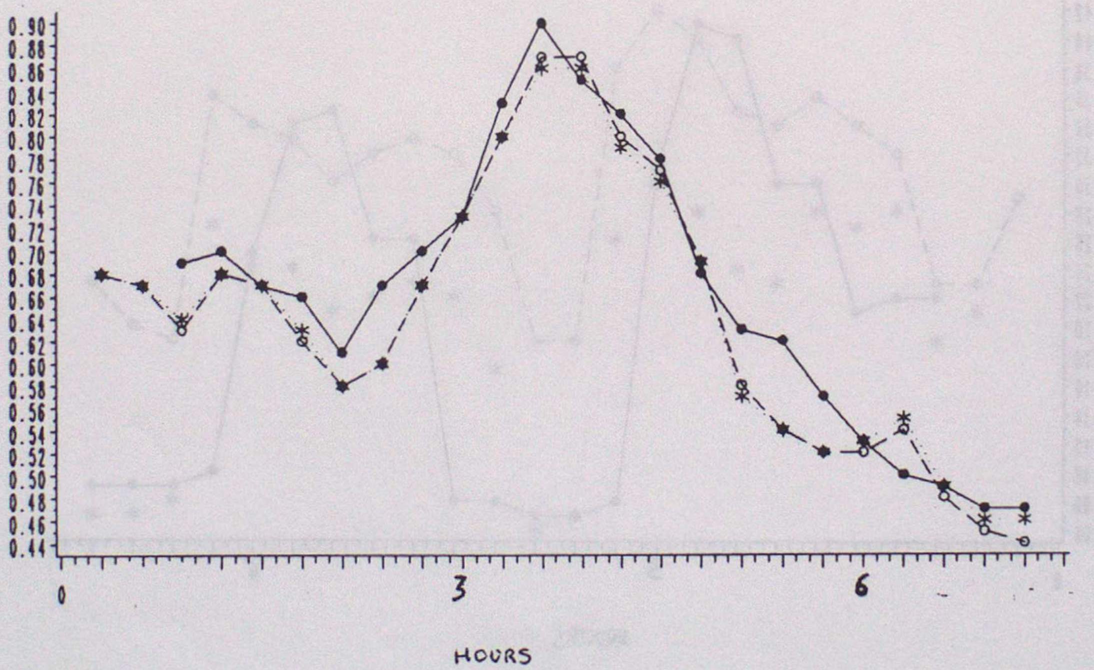

Fig. 7 Fit to P* and 10m winds during assimilation

KEY : stars - 'best run'
hollow circles - no synop winds
filled circles - original control

Plot of RMS (O-B) synop T increments from AC scheme - 4/12/91 case

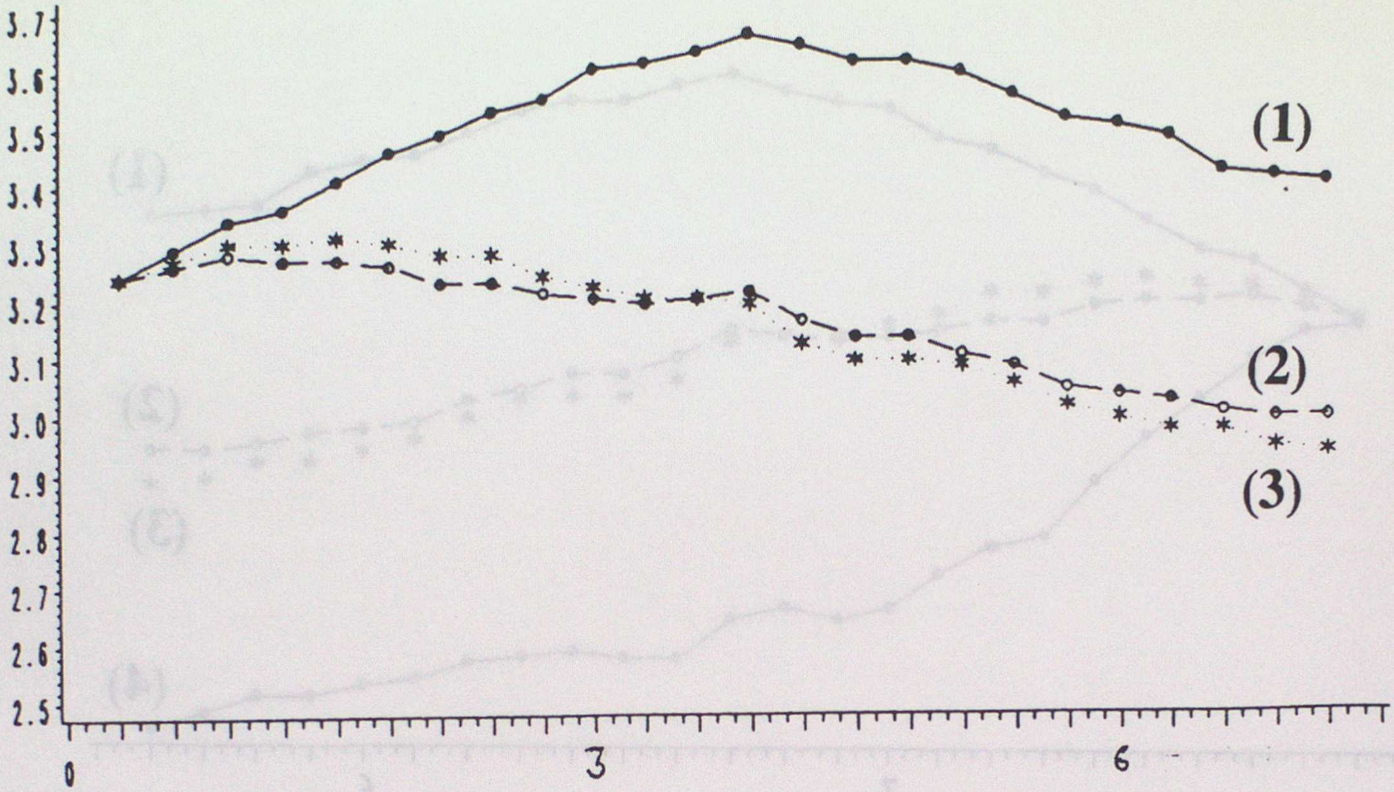

Plot of RMS (O-B) verification scores - 4/12/91 case

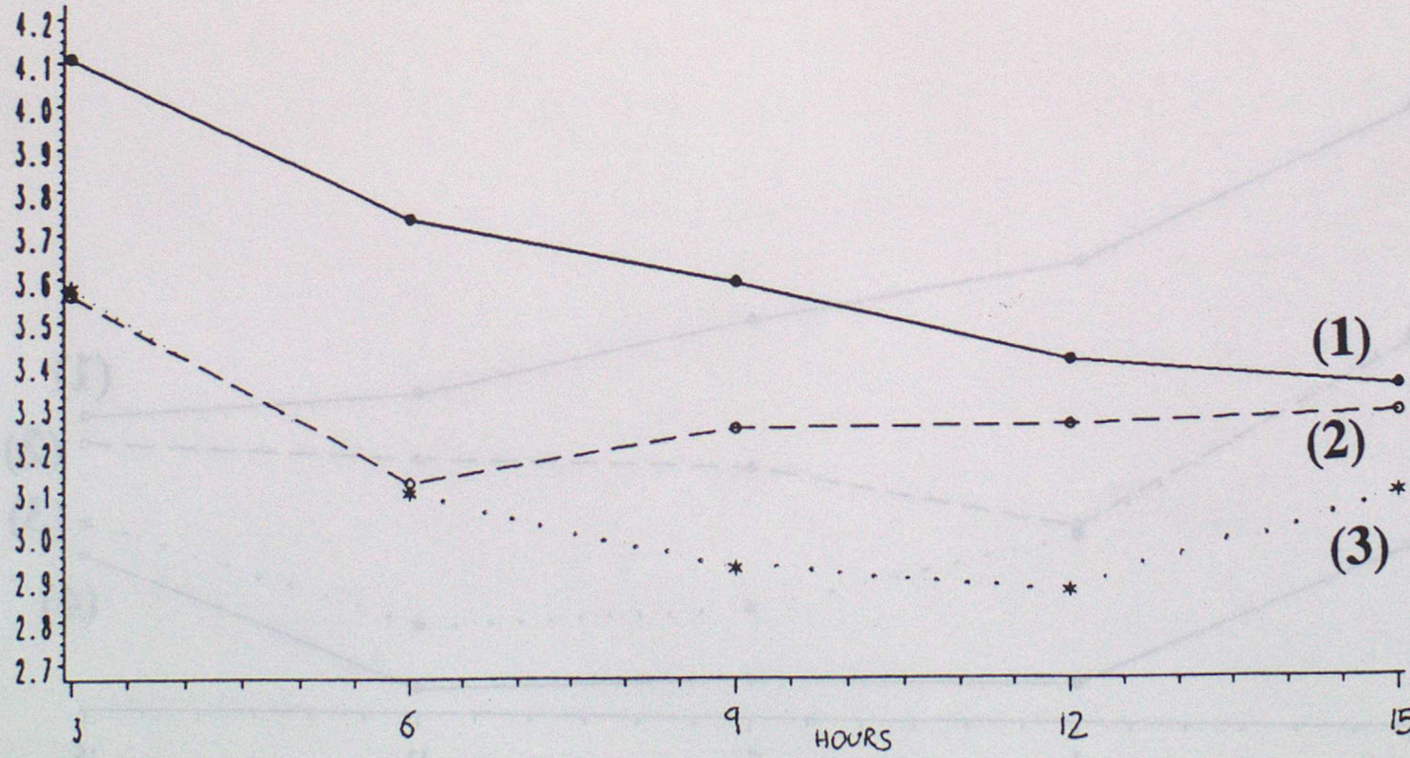

Fig. 8 Results from NMM runs with synop temperatures assimilated; (a) fit during assimilation ; (b) forecast verification scores.

KEY : (1) No synop temperatures
(2) Synop temperature increments added over 1 level
(3) Synop temperature increments added over 10 levels.

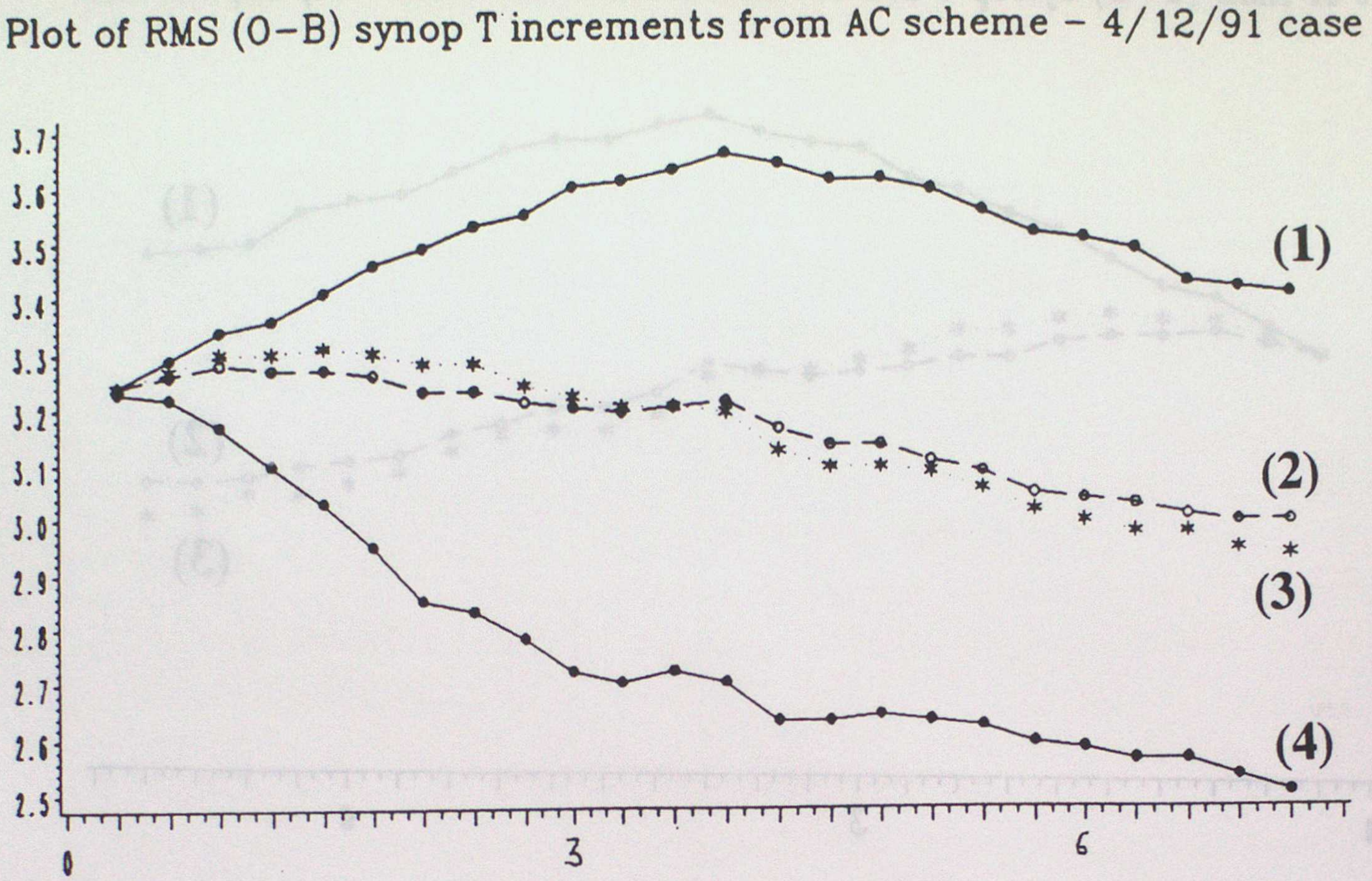

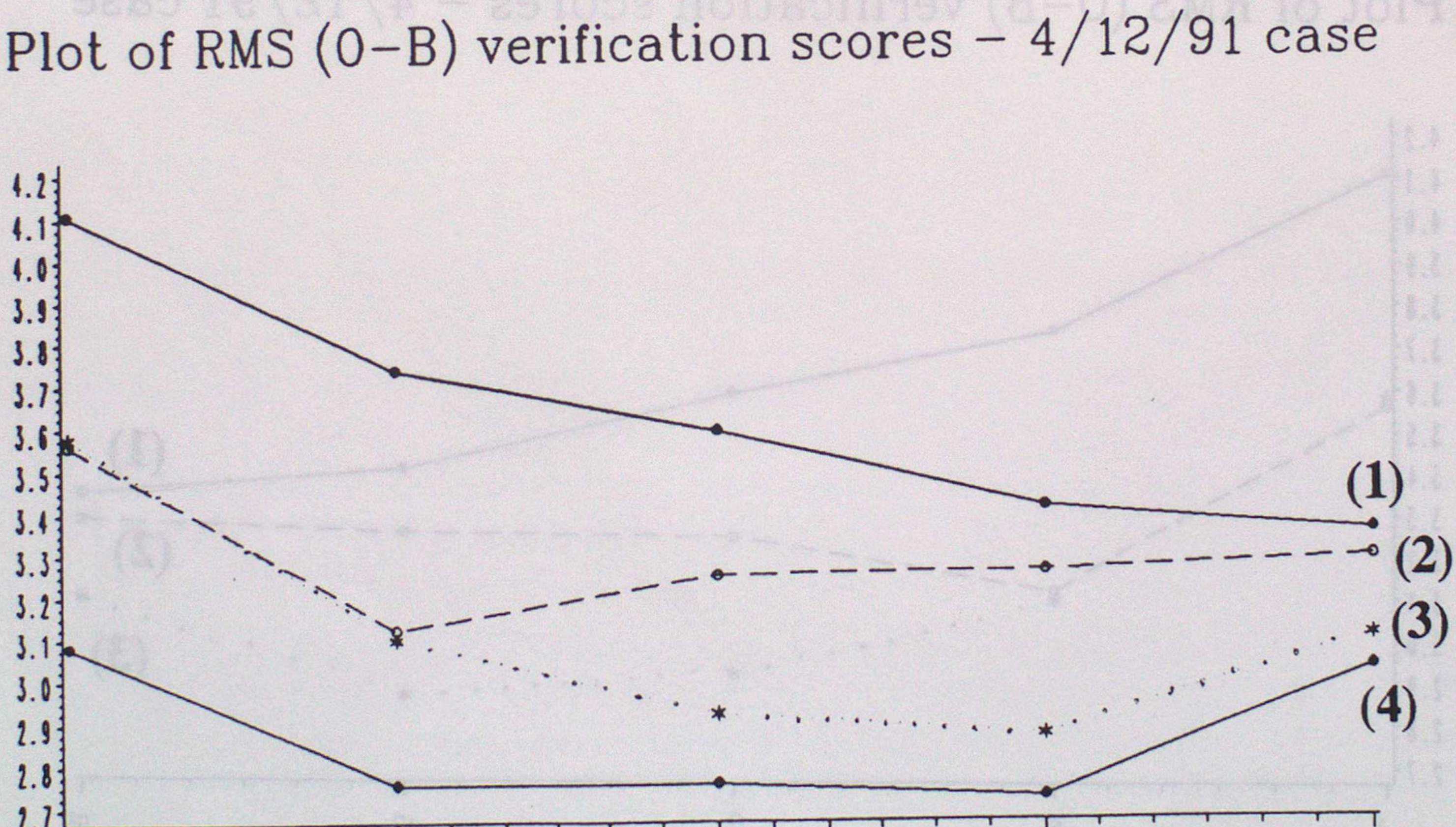

Fig. 9 As Fig.8 but with results from run in which the level 1 temperature increments were added to the T* field (curves 4).

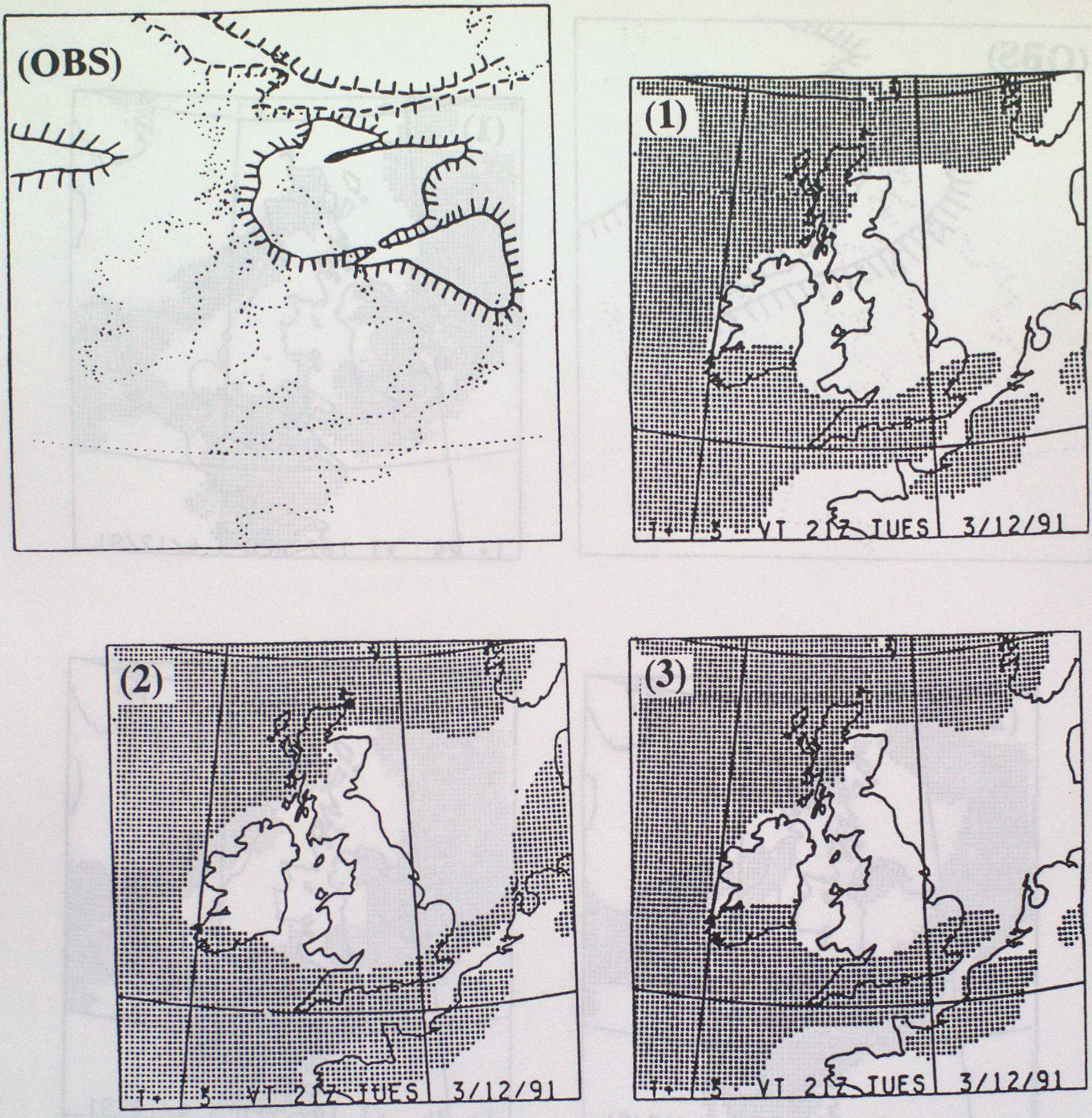

Fig. 10a Cloud forecasts valid at 3Z 3/12/1991 :

KEY : (1) No synop temperatures
(2) Synop temperature increments added over 10 levels
(3) Synop temperature increments added over 1 level

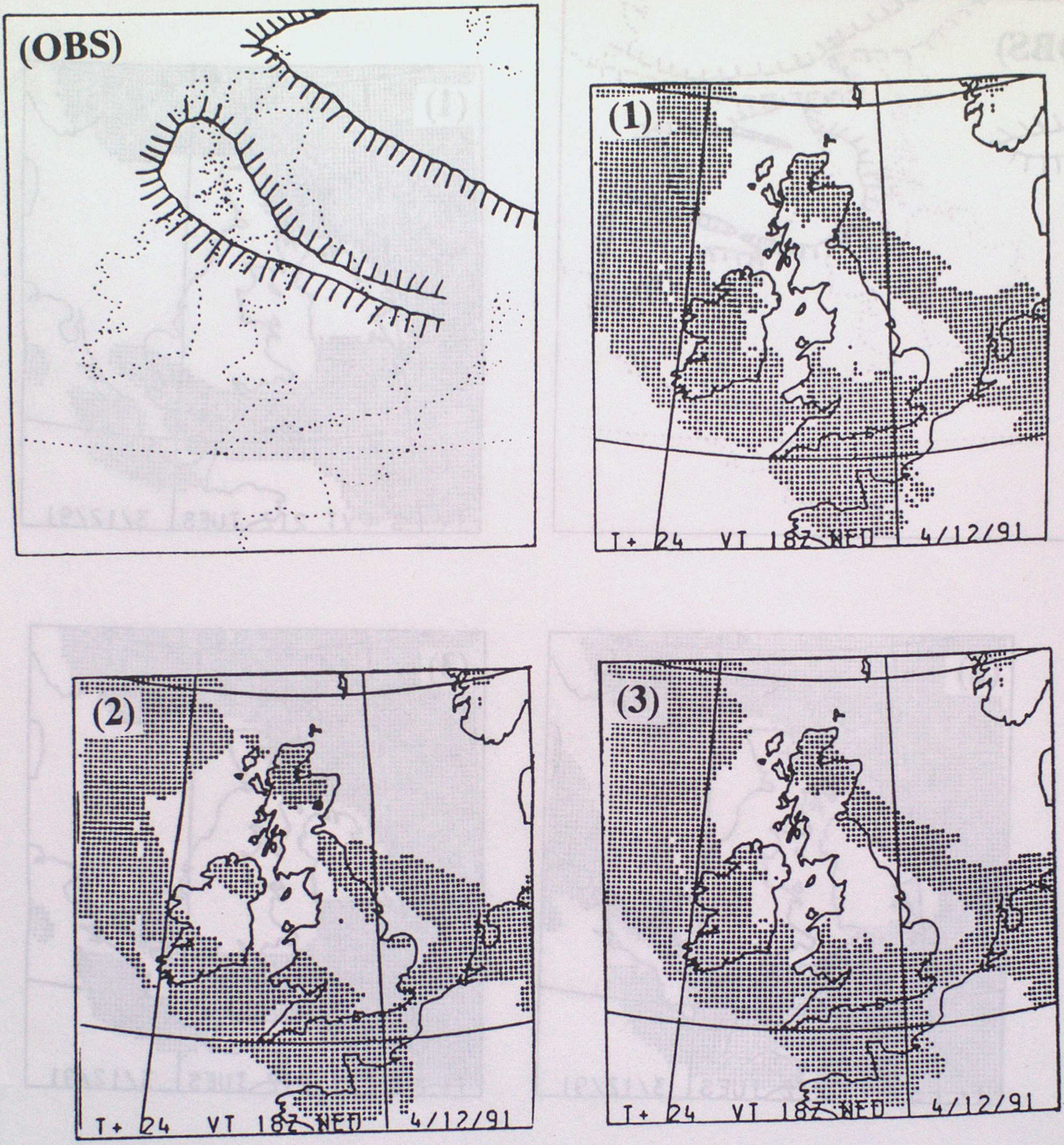

Fig. 10b Cloud forecasts valid at 18Z 4/12/1991 - see Fig. 10a for key.

VERTICAL CORRELATION COEFFICIENT (μv)

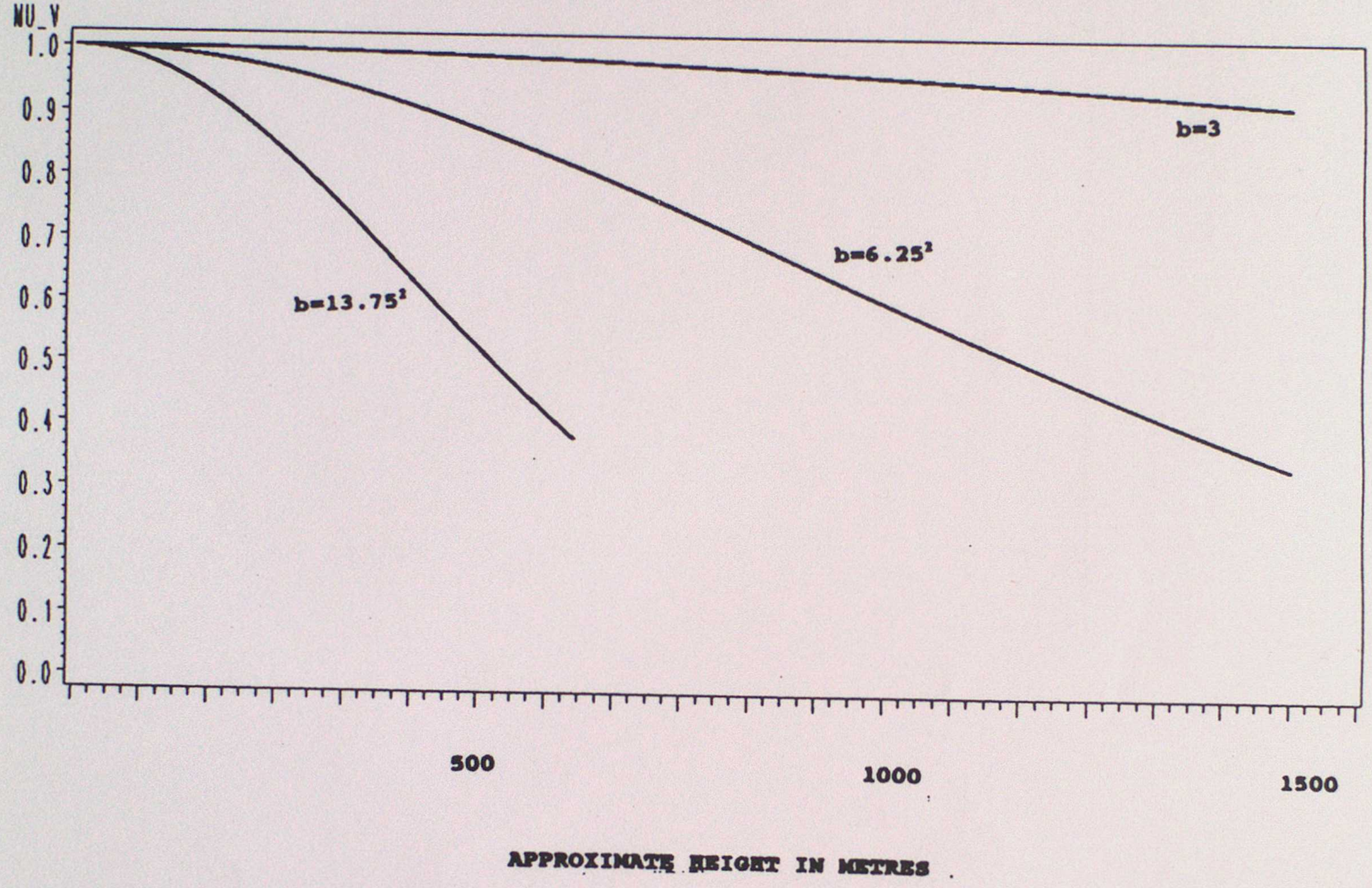

Fig. 11 The effect of increasing the value of 'b' on the vertical correlation coefficient.

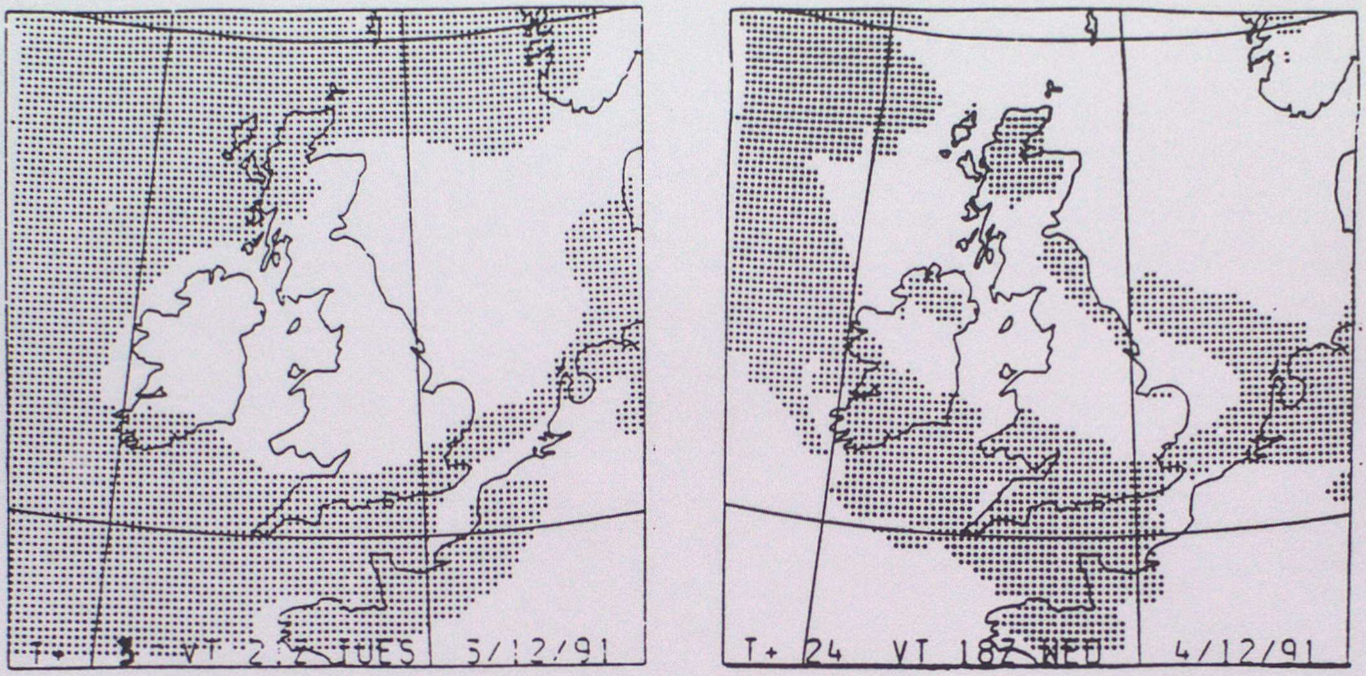

Fig. 12 Cloud forecasts resulting from sharper vertical correlation coefficient profile.

PARAMETER	VALUE
CORRELATION SCALE (C.S) (km)	(225/150/165)
TIME WINDOW (minutes)	(-120,24) (-150,30) for ship winds
RADIUS OF INFLUENCE (n X C.S)	1.75 2.5 for ship winds

Table 1. NMM surface data assimilation parameters used operationally.

Forecasting Research Division Technical Reports

Forecasting Research Division Technical Reports

1.	ON THE TIME SAVING THAT CAN BE ACHIEVED BY THE USE OF AN OPTIMISED COURSE IN AN AREA OF VARIABLE FLOW	R.W. Lunnon A.D. Marklow September 1991
2.	Treatment of bias in satellite sea surface temperature observations	R.S.Bell August 1991
3.	FINITE DIFFERENCE METHODS	M.J.P. Cullen August 1991
4.	Representation and recognition of convective cells using an object-orientated approach	W.H. Hand 30th September 1991
5.	Sea-ice data for the operational global model.	C.P.Jones November 1991.
6.	Tuning and Performance of the Atmospheric Quality Control.	N.B. Ingleby. December 1991.
7.	More satellite sounding data - can we make good use of it?	R.S.Bell January 1992.
8.	WAM/UKMO Wind Wave model Intercomparison Summary Report	Heinz Gunther ECMWF Martin Holt UK Met Office January 1992
9.	Spin up problems of the UKMO Mesoscale Model and moisture nudging experiments	Akihide Segami JMA February 1992
10.	A comparison of 2nd generation and 3rd generation wave model physics	M.W. Holt B.J. Hall February 1992
11.	RETRIEVAL AND ASSIMILATION: SYSTEM CONSIDERATIONS	Andrew C Lorenc March 1992
12.	Detection of Precipitation by Radars in the UK Weather Radar Network	M. Kitchen P.M. Brown April 1992
13.	THE VALUE OF WIND OBSERVATIONS FOR WEATHER FORECASTING AND CLIMATE STUDIES	Andrew C Lorenc April 1992
14.	An investigation into the parameters used in the analysis scheme of the Mesoscale Model	G. Veitch B.J. Wright S.P Ballard May 1992
15.	THE VERIFICATION OF MESOSCALE MODEL FORECASTS OF LIQUID WATER CONTENT USING HELICOPTER REPORTS OVER THE NORTH SEA DURING WINTER 1991	M. Ahmed R.W Lunnon R.J. Graham May 1992

Forecasting Research Division Technical Reports

16.	Simulations of the Diurnal Evolution of Marine Stratocumulus Part I: The sensitivity of the Single Column Version of the Mesoscale Model to Changes in the . Turbulence Scheme.	S.D.Jackson S.P. Ballard May 1992
17.	Simulations of the Diurnal Evolution of Marine Stratocumulus Part II: A Comparison of Radiation Schemes Using the Single Column Version of the Mesoscale Model.	S.D.Jackson S.P. Ballard May 1992
18.	Quantifying the low level windshear aviation hazard for the UK: some research proposals	R.J. Graham R.W. Lunnon May 1992
19.	WAM/UKMO Wind Wave model Intercomparison Part 2 Running the UKMO wave model at higher resolution	M.W. Holt April 1992
20.	Sensitivity of Mesoscale Model forecasts of anticyclonic Statocumulus to the specifications of initial conditions and Boundary Layer mixing scheme.	B.J. Wright S.P. Ballard July 1992
21.	Evaluation of diffusion and gravity wave changes in the Global Forecast Model.	F. Rawlins O. Hammon 16 June 1992
22.	Background Errors for the Quality Control and Assimilation of Atmospheric Observations in the Unified Model - the situation in July 1992.	C.A. Parrett July 1992
23.	Estimation of the Mean and Standard Deviation of the Random Component of Data also Containing Non- random Errors.	B.R. Barwell July 1992
24.	Experiments in Nowcasting convective rain using an object- oriented approach.	W.H. Hand 15th August 1992
25.	Gravity Wave Speeds from the Eigenmodes of the Unified Model.	I. Roulstone 28 July 1992
26.	A re-calibration of the Wave Model	M.W. Holt August 1992
27.	Evaluation of Koistinen's method of radar range and bright band correction	A.G. Davies August 1992
28.	A Study of the Boundary Layer in the Mesoscale Unified Model	Graham Veitch August 21,1992
29.	Profiles of wind using time-sequences of absorption channel imagery from geostationary satellites: proof of concept using synthetic radiances	R.W.Lunnon September 1992
30.	AN EMPIRICAL INVESTIGATION OF THE "WATER VAPOUR TEMPERATURE LAPSE-RATE FEEDBACK" TO THE GREENHOUSE EFFECT	K.F.A. Smith R.J. Allam J.S.Foot September 1992
31.	Observation needs for operational ocean modelling	S.J. Foreman September 1992

Forecasting Research Division Technical Reports

32.	Bright band correlations for layered precipitation; the comparison of Chilbolton radar data and Hardaker model output.	A.G. Davies November 1992
33.	Progress and performance of the operational mesoscale model	S.P. Ballard
34.	Assessment of the bias of significant wave height in the Met.Office global wave model	S.J. Foreman M.W. Holt S. Kelsall
35.	STUDY OF CIRRUS CLOUD WINDS: ANALYSIS OF I.C.E DATA FINAL REPORT FOR EUMETSAT CONTRACT ITT 91/16	R.W. Lunnon D.A. Lowe J.A. Barnes I. Dharssi December 1992
36.	Revisions to the operational data assimilation-Nov.92	R.S. Bell January 1993
37.	A comparison of wind observations from a flight of the DRA(B)BAC 1-11 research aircraft over Hemsby, 11 June 1991, with observations from the Hemsby radiosonde	R.J. Graham January 1993
38.	The Moisture Observation Pre-processing System	B.J. Wright January 1993
39.	Performance of the data assimilation scheme in the operational trial of the new mesoscale model.	B. Macpherson B.J. Wright A.J. Maycock January 1993
40.	Development and performance of the new mesoscale model.	S.P. Ballard B. Robinson January 1993
41.	A PRELIMINARY ASSESSMENT OF OCEAN SURFACE FLUXES FROM UNIFIED MODEL FORECASTS	J.O.S. Alves S.J.Foreman M.W. Holt S. Kelsall S.J.Nightingale January 1993
42.	Some notes on primitive and quasi-equilibrium equations with a hybrid vertical coordinate and remarks on Hamiltonian structure.	I.Roulstone 23rd March 1993
43.	Development of the surface data assimilation scheme for the new mesoscale model	A.J. Maycock April 1993
44.	A REVIEW OF SEA ICE MODELS FOR USE IN FOAM	C.G. Sherlock April 1993